OPEN ACCESS

Original research

Squalene epoxidase drives cancer cell proliferation and promotes gut dysbiosis to accelerate colorectal carcinogenesis

Chuangen Li,[1] Yong Wang,[2] Dabin Liu,[1] Chi Chun Wong,[1] Olabisi Oluwabukola Coker,[1] Xiang Zhang,[1] Changan Liu,[1] Yunfei Zhou,[1] Yali Liu,[1] Wei Kang ,[3] Ka Fai To,[3] Joseph JY Sung ,[4] Jun Yu [1]

► Additional supplemental material is published online only. To view, please visit the journal online (http://dx.doi.org/10.1136/gutjnl-2021-325851).

For numbered affiliations see end of article.

Correspondence to
Dr Jun Yu, Department of Medicine and Therapeutics, The Chinese University of Hong Kong, Hong Kong, Hong Kong; junyu@cuhk.edu.hk

CL and YW are joint first authors.

Received 10 August 2021
Accepted 15 February 2022
Published Online First 1 March 2022

ABSTRACT

Objective Aberrant lipid metabolism is a hallmark of colorectal cancer (CRC). Squalene epoxidase (SQLE), a rate-limiting enzyme in cholesterol biosynthesis, is upregulated in CRC. Here, we aim to determine oncogenic function of SQLE and its interplay with gut microbiota in promoting colorectal tumourigenesis.

Design Paired adjacent normal tissues and CRC from two cohorts were analysed (n=202). Colon-specific Sqle transgenic (Sqle tg) mice were generated by crossing Rosa26-lsl-Sqle mice to Cdx2-Cre mice. Stools were collected for metagenomic and metabolomic analyses.

Results SQLE messenger RNA and protein expression was upregulated in CRC ($p<0.01$) and predict poor survival of patients with CRC. SQLE promoted CRC cell proliferation by inducing cell cycle progression and suppressing apoptosis. In azoxymethane-induced CRC model, Sqle tg mice showed increased tumourigenesis compared with wild-type mice ($p<0.01$). Integrative metagenomic and metabolomic analyses unveiled gut dysbiosis in Sqle tg mice with enriched pathogenic bacteria, which was correlated to increased secondary bile acids. Consistent with detrimental effect of secondary bile acids, gut barrier function was impaired in Sqle tg mice, with reduced tight junction proteins Jam-c and occludin. Transplantation of Sqle tg mice stool to germ-free mice impaired gut barrier function and stimulated cell proliferation compared with control mice stool. Finally, we demonstrated that terbinafine, a SQLE inhibitor, could be repurposed for CRC by synergising with oxaliplatin and 5-fluorouracil to inhibit CRC growth.

Conclusion This study demonstrates that SQLE mediates oncogenesis via cell intrinsic effects and modulation of gut microbiota-metabolite axis. SQLE represents a therapeutic target and prognostic marker in CRC.

Significance of this study

What is already known on this subject?

⇒ Aberrant lipid metabolism is a hallmark in colorectal cancer (CRC).

⇒ Cholesterol metabolism is frequently upregulated in CRC, but its function and potential interaction with gut microbiome remains unknown.

What are the new findings?

⇒ Squalene epoxidase (SQLE) is overexpressed in CRC and its high expression predicts poor survival.

⇒ Colon-specific *Sqle* transgenic expression in mice promotes colorectal tumourigenesis in azoxymethane-induced CRC.

⇒ Integrative metagenomic and metabolomic analyses demonstrate that colon-specific *Sqle* transgenic mice harbours a dysregulated microbiome with enriched pathogenic bacteria, which is correlated to increased secondary bile acids production.

⇒ Gut barrier function is disrupted in Sqle transgenic mice with suppressed tight junction proteins Jam-c and occludin.

⇒ Faecal transplantation of Sqle transgenic mice stool into germ-free mice promotes colonic cell proliferation and gut barrier disruption.

⇒ SQLE inhibitor terbinafine synergises with chemotherapy to inhibit CRC growth in vitro and in vivo.

How might it impact on clinical practice in the foreseeable future?

⇒ Targeting of SQLE-gut microbiome axis is a potential strategy for CRC prevention and treatment.

INTRODUCTION

Colorectal cancer (CRC) is the third most common cancer and ranks the second in terms of cancer mortality worldwide. Both the incidence and mortality of CRC are still increasing in young people, especially in low-income and middle-income countries. Patients with advanced CRC with metastasis still suffer from poor prognosis and drug resistance severely diminishes the therapeutic efficacy of chemotherapy. Hence, it is important to identify novel genes involved in the pathogenesis of CRC in order to develop effective treatments, either alone or in combination with chemotherapy.

Aberrant lipid metabolism is increasingly considered a hallmark characteristic of many cancers, including CRC. Both obesity and serum lipids are risk factors for CRC.[1 2] Epidemiological studies also

Check for updates

To cite: Li C, Wang Y, Liu D, *et al*. *Gut* 2022;**71**:2253–2265.

suggest a high dietary fat intake to increased risk of CRC.[3] Lipid accumulation promotes CRC through increased reactive oxygen species and MAPK signalling.[4] Fatty acids,[5 6] cholesterol[7 8] and bile acids[9] have been implicated in CRC pathogenesis. Nevertheless, lipid metabolism-dependent molecular mechanisms involved in CRC remains poorly understood.

Squalene epoxidase (SQLE) is a rate-limiting enzyme in cholesterol biosynthesis. Recent work has shown that SQLE is overexpressed in CRC[8 10 11]; nevertheless, the potential role of SQLE in CRC initiation and progression remains controversial. SQLE was suggested to be oncogenic factor by promoting cell growth,[10] whereas Jun *et al*[8] showed that reduction of SQLE could accelerate CRC metastasis. In this study, we demonstrated that SQLE is upregulated in CRC compared with adjacent normal tissues in multiple CRC cohorts and predicts poor patient survival.

To comprehensively decipher the role of SQLE in CRC, we first established colon-specific SQLE transgenic (tg) mice and SQLE knockout (KO) mice, we demonstrated the role of SQLE as an oncogene in CRC in vivo. We revealed that colon-specific SQLE overexpression promoted gut dysbiosis and metabolic alterations, which contribute to impaired gut barrier and induced colonic cell proliferation. Finally, we showed terbinafine, a Food and Drug Administration (FDA)-approved inhibitor of SQLE, synergised with 5-fluorouracil (5-FU) or oxaliplatin to inhibit the growth of CRC cells in vitro and in vivo. These findings suggest SQLE as a targetable oncogenic factor in CRC.

MATERIALS AND METHODS

Human CRC samples

Patient samples (Hong Kong cohort) with histologically confirmed CRC were collected in Beijing University Cancer Hospital when patients underwent surgery (n=144). Both tumour and adjacent normal tissues were immediately snap-frozen in liquid nitrogen. Patient characteristics are summarised in online supplemental table S1. An additional tissue microarray (TMA) cohort consists of 207 patients with CRC who underwent surgery in Prince of Wales Hospital, Hong Kong. The patient characteristics are summarised in online supplemental table S2. A publicly available cohort (GSE17538) was used for validation, containing 232 patients with CRC (online supplemental table S3). The Cancer Genome Atlas (TCGA) cohort dataset was accessed from UCSC Xena browser (https://xenabrowser.net/), with 50 paired adjacent normal and tumour samples from RNA-sequencing. GDS4382 consists of 17 paired adjacent normal and tumour samples analysed by the Affymetrix Human Genome U133 Plus 2.0 Array (https://www.ncbi.nlm.nih.gov/sites/GDSbrowser?acc=GDS4382).

Colon-specific Sqle transgenic mice model

Sqle tg mice (Rosa26-pCAG-loxp-stop-loxp-SQLE) were previously established by us.[12] To drive the colon-specific expression of SQLE, Sqle tg mice were crossed to Cdx2-Cre^{ERT2} mice. To activate SQLE overexpression, tamoxifen (100 mg/kg, intraperitoneally) was first injected to Sqle tg mice aged 6 weeks for 4 times daily to activate Cre^{ERT2}. To induce colorectal carcinogenesis in Sqle tg mice, we employed the chemically induced CRC model. Briefly, azoxymethane (AOM, 10 mg/kg, intraperitoneally) was administered into mice 6 times, once per week. Mice were then sacrificed at week 24 after the first AOM injection. The number and size of tumours were recorded. All tissues were immediately stored in 10% formalin or −80°C freezer. Histology was scored after H&E staining by a pathologist blinded to the nature of samples.

Sqle knockout mice model

Whole body Sqle KO mice were generated by CRISPR/Cas9 technology. Heterozygous Sqle KO mice (Sqle$^{+/-}$ mice) were employed for the AOM-Dextran sulfate sodium (DSS) model, as homozygous KO mice were not viable. To induce CRC, Sqle$^{+/-}$ and wild-type mice were injected once with AOM (10 mg/kg, intraperitoneally) at 6 weeks of age. One week after AOM injection, three cycles of DSS treatment (2% in drinking water for 5 days) were given, with 2 weeks of break between each cycle. Mice were sacrificed 80 days after the first AOM injection. The number and size of tumours were measured. All tissues were immediately stored in 10% formalin or −80°C freezer.

Xenograft models

SW1116 and LOVO cells expressing empty vector or SQLE plasmid (1×10^7 cells in 0.1 mL phosphate-buffered saline (PBS)) were injected subcutaneously into the left dorsal flank of Balb/c nude mice aged 4 weeks. Subcutaneous tumour size was measured with a digital calliper. After 4 weeks, mice were sacrificed and examined. For drug treatment study, HT29 cells (1×10^7 cells in 0.1 mL PBS) were injected subcutaneously to dorsal flank of nude mice. The mice were randomised and received: (1) vehicle; (2) terbinafine (80 mg/kg, orally, daily); (3) 5-FU (30 mg/kg, intraperitoneally, 2 times per week); (4) oxaliplatin (10 mg/kg, intraperitoneally, once per week); (5) terbinafine+5-FU and (6) terbinafine+oxaliplatin. Tumour size was monitored and mice were sacrificed after 4 weeks.

In vivo intestinal permeability assay

To determine in vivo intestinal permeability, mice were starved overnight and fluorescein isothiocyanate (FITC)-dextran (Sigma) was administered by oral gavage (44 mg/100 g body weight). After 4 hours, mice were anaesthetised, blood was collected by cardiac puncture and mice were sacrificed. The serum was separated from whole blood, diluted and FITC fluorescence was then determined by spectrophotofluorometry (BioTek), with an excitation and emission of 485 nm and 528 nm, respectively. Serially diluted FITC-dextran was used as standard.

Shot-gun metagenome sequencing

Stool was collected from Sqle tg mice and wild-type littermates, and extracted using PowerFecal DNA isolation kit. Nextera XT adapter was used to generate amplified library, and sequencing was performed to obtain DNA (125 bp) paired end reads to a depth of 10G base pairs per sample using HiSeq Illuminex 2500. The same annotation pipeline was used for all faecal metagenomes in this study. For data analysis, host DNA removal and reads quality filtering were performed by BWA and SAM tools.[13 14] After that, high-quality reads were used to obtain species-level taxonomic profiling by Kraken2 and Bracken.[15 16] The differential abundance of species-level bacteria was performed by R package DESeq2.[17] Bacteria species with adjusted $p<0.05$ and log2(fold change) >1 were considered statistically significant. Principal coordinate analysis was conducted using R packages phyloseq and vegan.[18]

Statistical analysis

All statistical tests were performed using SPSS (Version 19.0) or GraphPad Software. Data are presented as mean±SD. Cell viability assay and tumour growth rate evaluation was analysed with repeated-measures analysis of variance. The effect of clinical characteristics on SQLE messenger RNA (mRNA) expression and comparison between two groups was analysed with paired

two-tailed Student's t-test. The effect of clinical characteristics on SQLE protein expression was analysed with Pearson's χ^2 test or Fisher's exact test. To evaluate the correlation between SQLE and prognosis, overall survival (OS) was defined as the duration from the date of surgery to the date of death. Using the Kaplan-Meier analysis, OS curve was formulated. Multivariate analysis for OS was performed with Cox proportional hazard regression analysis. To determine the significance SQLE on OS, log-rank test was used. P values <0.05 were considered statistically significant.

Additional methods are provided in online supplemental information.

RESULTS

SQLE is overexpressed in patients with CRC

We analysed mRNA expression of SQLE in three independent CRC cohorts (in-house Hong Kong cohort, TCGA and GDS4382). The clinical characteristics of Hong Kong cohort are shown in online supplemental table S1. SQLE mRNA was highly upregulated in primary CRC as compared with adjacent normal tissues (n=141, p<0.0001), as determined by quantitative PCR (qPCR) (figure 1A). SQLE mRNA expression demonstrated significant correlation with advanced tumour, node, metastases stage (p<0.05) and distant metastasis (p<0.05) (online supplemental table S1). Its overexpression was validated in TCGA (n=50; p<0.0001) and GDS4382 cohorts (n=17; p<0.001) (figure 1A). At protein level, immunohistochemistry (IHC) validated overexpression of SQLE protein in CRC tumours compared with adjacent normal tissues (p<0.01) (figure 1B). Hence, SQLE overexpression is a frequent event in CRC.

SQLE overexpression is associated with poor prognosis in patients with CRC

Given its frequent overexpression in CRC, we then assessed the clinical significance of SQLE in human CRC. In Hong Kong cohort, Kaplan-Meier curve showed that high SQLE mRNA levels were associated with poor survival in patients with CRC (p<0.05) (figure 1C). Consistently, multivariate Cox proportional hazards regression analysis revealed that high SQLE mRNA expression was an independent prognostic factor associated with poor disease-specific survival in patients with CRC (p<0.05; HR 1.832; 95% CI 1.113 to 3.113) (figure 1C). We validated the prognostic significance of SQLE mRNA in GSE17538 cohort (n=232) (online supplemental table S3) using Kaplan-Meier curve (p<0.05) and univariate Cox proportional hazards regression analysis (p<0.05) (figure 1D).

To determine whether SQLE predicts patient prognosis at protein level, we performed TMA analysis of 207 CRC cases by IHC (figure 1E). Evaluation of clinical characteristics with respect to SQLE protein levels revealed significant associations with The American Joint Committee on Cancer stage (p<0.01), lymph node metastasis (p<0.01) and distant metastasis (p<0.001) (online supplemental table S2), implying that SQLE may be involved in tumour progression. Indeed, high SQLE protein expression was associated with poor survival in patients with CRC by Kaplan-Meier curve (p<0.001) analysis (figure 1E) and by multivariate Cox proportional hazards regression analysis (p<0.05; HR 1.951; 95% CI 1.225 to 2.391) (figure 1E). Our data collectively indicate that SQLE mRNA and protein expression are independent prognostic factors for predicting poor survival of patients with CRC.

SQLE promotes CRC cell growth

To determine the oncogenic effect of SQLE in human CRC, we overexpressed SQLE in CRC cells LOVO and SW1116 (figure 2A) with low endogenous SQLE levels (online supplemental figure S1). SQLE expression promoted cell growth, as evidenced by both cell growth curve (p<0.01) (figure 2A) and colony formation assay (p<0.01) (figure 2B). Conversely, we performed SQLE knockdown in CRC cells HT29 and DLD1 (online supplemental figure S1), with high endogenous SQLE expression (figure 2C). SQLE short hairpin (sh) RNA suppressed cell viability (p<0.01) (figure 2C) and colony formation (p<0.01) (figure 2D) compared with shControl cells. Next, tumourigenic effect of SQLE were investigated in nude mice model. LOVO and SW1116 cells stably expressing empty vector or SQLE were injected subcutaneously into left and right dorsal flanks of nude mice, respectively. As shown in figure 2E, SQLE overexpression markedly increased tumour volume of LOVO (p<0.01) and SW1116 (p<0.01) xenografts. SQLE depletion also suppressed proliferation of primary CRC-derived organoids (figure 2F). Together, SQLE promotes CRC cell growth in vitro and in vivo.

SQLE suppresses apoptosis and promotes cell cycle progression in CRC cell lines

We next determined the cytokinetic effect of SQLE in CRC cell lines. Overexpression of SQLE in LOVO and SW1116 cells suppressed apoptosis, as determined by annexin V/7-aminoactinomycin D assay (figure 3A). Inhibition of apoptosis by SQLE was further evidenced by reduced protein expression of cleaved (active) forms of caspase-3, caspase-7 and poly ADP-ribose polymerase (PARP) in SQLE-expressing SW1116 and LOVO cells (figure 3B). Conversely, SQLE knockdown promoted the induction of apoptosis in HT29 and DLD1 cells (figure 3C), together with increased cleaved caspase-3, caspase-7 and PARP (figure 3D). We analysed cell cycle distribution by flow cytometry, and showed that SQLE overexpression LOVO and SW1116 cells increased S phase population, with a concomitant decrease in cells in G1 phase (figure 3E). Consistent with this observation, SQLE overexpression increased the protein expression of proliferating cell nuclear antigen (PCNA), cyclin D1 and CDK4, but suppressed expression of cell cycle inhibitors $p21^{Cip1}$, $p27^{Kip1}$ and p53 (figure 3F). In contrast, SQLE knockdown in HT29 and DLD1 cells induced G1 cell cycle arrest (figure 3G), implying that SQLE accelerated G1-S progression. SQLE knockdown suppressed PCNA, cyclin D1 and CDK4, while promoting the expression of cell cycle inhibitors (figure 3H). Collectively, SQLE promotes CRC growth by inhibiting apoptosis and activating cell cycle progression.

Colon-specific transgenic SQLE expression in mice accelerates colorectal tumourigenesis

To determine the relevance of SQLE in colorectal tumourigenesis in vivo, we constructed colon-specific Sqle tg mice by crossing Rosa26-Sqle tg mice to Cdx2-Cre^{ERT2} mice (figure 4A). Colon-specific overexpression of Sqle was activated with tamoxifen injection, which allows the activation of Cre the in colon epithelium (figure 4B). To initiate colorectal tumourigenesis, we injected wild-type and Sqle tg mice with 10 mg/kg AOM once a week for a total of 6 weeks (figure 4B). At 180 days after the first AOM injection, mice were sacrificed and the colon was analysed. As shown in figure 4C, Sqle tg mice demonstrated increased tumour incidence (10/10 vs 6/10), tumour number (p<0.01) and tumour burden (p<0.01) as compared with wild-type mice, implying an

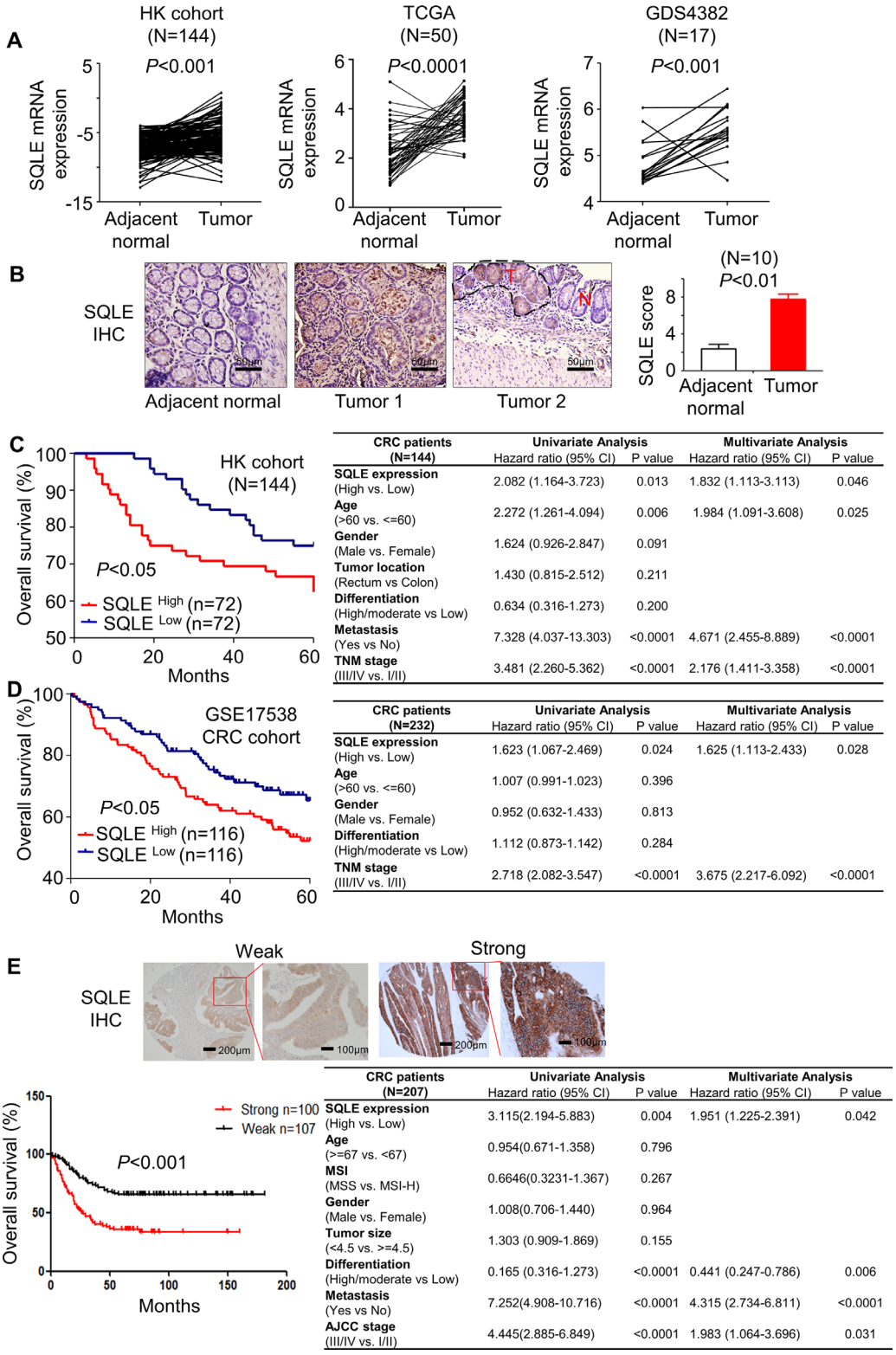

CRC patients (N=144)	Univariate Analysis Hazard ratio (95% CI)	P value	Multivariate Analysis Hazard ratio (95% CI)	P value
SQLE expression (High vs. Low)	2.082 (1.164-3.723)	0.013	1.832 (1.113-3.113)	0.046
Age (>60 vs. <=60)	2.272 (1.261-4.094)	0.006	1.984 (1.091-3.608)	0.025
Gender (Male vs. Female)	1.624 (0.926-2.847)	0.091		
Tumor location (Rectum vs Colon)	1.430 (0.815-2.512)	0.211		
Differentiation (High/moderate vs Low)	0.634 (0.316-1.273)	0.200		
Metastasis (Yes vs No)	7.328 (4.037-13.303)	<0.0001	4.671 (2.455-8.889)	<0.0001
TNM stage (III/IV vs. I/II)	3.481 (2.260-5.362)	<0.0001	2.176 (1.411-3.358)	<0.0001

CRC patients (N=232)	Univariate Analysis Hazard ratio (95% CI)	P value	Multivariate Analysis Hazard ratio (95% CI)	P value
SQLE expression (High vs. Low)	1.623 (1.067-2.469)	0.024	1.625 (1.113-2.433)	0.028
Age (>60 vs. <=60)	1.007 (0.991-1.023)	0.396		
Gender (Male vs. Female)	0.952 (0.632-1.433)	0.813		
Differentiation (High/moderate vs Low)	1.112 (0.873-1.142)	0.284		
TNM stage (III/IV vs. I/II)	2.718 (2.082-3.547)	<0.0001	3.675 (2.217-6.092)	<0.0001

CRC patients (N=207)	Univariate Analysis Hazard ratio (95% CI)	P value	Multivariate Analysis Hazard ratio (95% CI)	P value
SQLE expression (High vs. Low)	3.115(2.194-5.883)	0.004	1.951 (1.225-2.391)	0.042
Age (>=67 vs. <67)	0.954(0.671-1.358)	0.796		
MSI (MSS vs. MSI-H)	0.6646(0.3231-1.367)	0.267		
Gender (Male vs. Female)	1.008(0.706-1.440)	0.964		
Tumor size (<4.5 vs. >=4.5)	1.303 (0.909-1.869)	0.155		
Differentiation (High/moderate vs Low)	0.165 (0.316-1.273)	<0.0001	0.441 (0.247-0.786)	0.006
Metastasis (Yes vs No)	7.252(4.908-10.716)	<0.0001	4.315 (2.734-6.811)	<0.0001
AJCC stage (III/IV vs. I/II)	4.445(2.885-6.849)	<0.0001	1.983 (1.064-3.696)	0.031

Figure 1 Squalene epoxidase (SQLE) is upregulated in colorectal cancer (CRC) and its expression predicts poor survival. (A) SQLE messenger RNA (mRNA) expression was determined in paired tumour and adjacent normal tissues from Hong Kong (HK) cohort (Beijing, n=144), The Cancer Genome Atlas (TCGA) cohort (n=50) and the GDS4382 cohort (n=17). Paired two-tailed Student's t-test was used to calculate p value. (B) SQLE protein expression was determined in paired tumour and adjacent normal tissues (n=10) by immunohistochemistry (IHC). Paired two-tailed Student's t-test was used to calculate p value. Scale bars, 50 µm. (C) Kaplan-Meier curve analysis revealed that patients with CRC with high SQLE mRNA has significantly lower 5-year survival as compared with patients with low SQLE mRNA in HK cohort (left). Cox regression analysis (right). (D) SQLE mRNA expression is associated with poor survival by Kaplan-Meier curve (left) and Cox regression analysis (right) in GSE17538 cohort. (E) Tissue microarray (TMA) analysis demonstrated that patients with CRC with high SQLE protein expression have significantly lower 5-year survival, as evidenced by Kaplan-Meier curve (left) and Cox regression analysis (right). Nuclear staining of 10% was used as the cut-off value. *P<0.05; **p<0.01; ***p<0.001. AJCC, The American Joint Committee on Cancer; TNM, tumour, node, metastases.

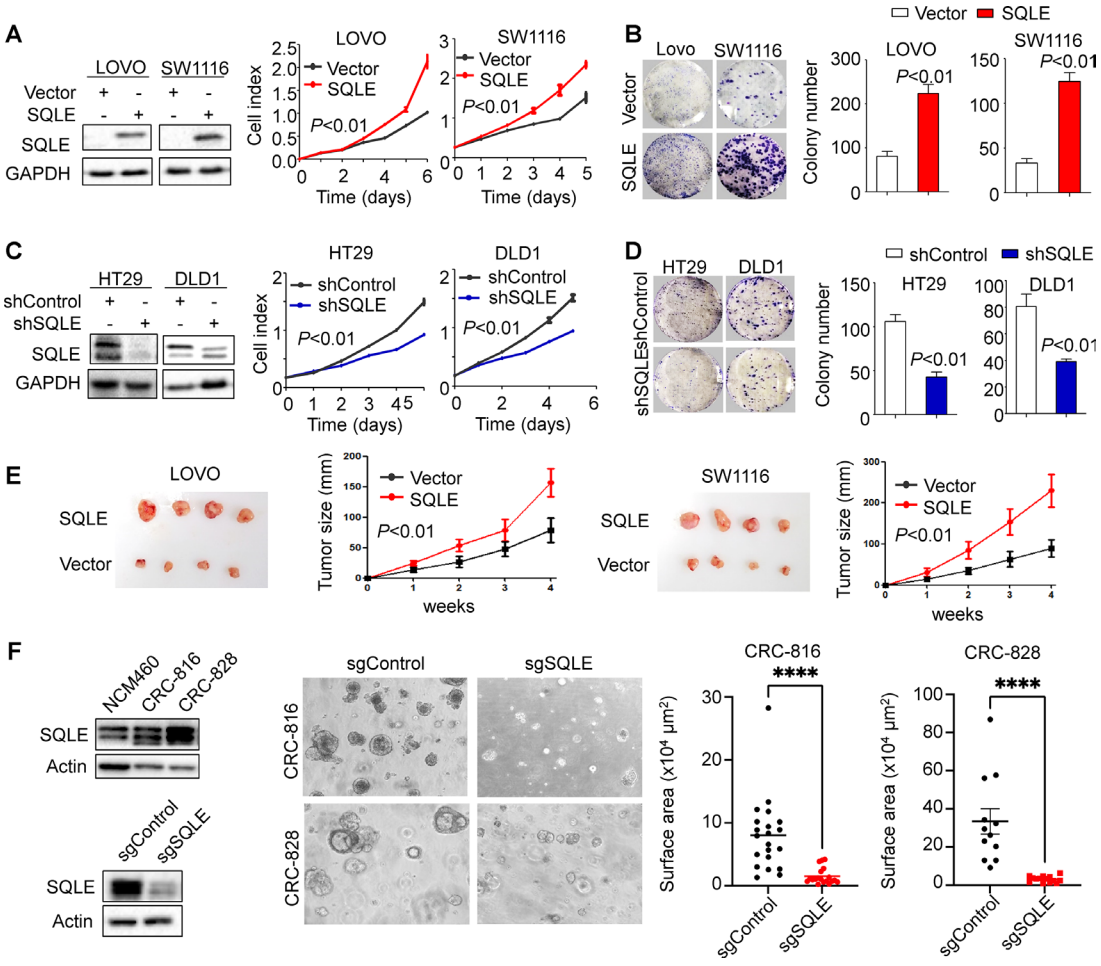

Figure 2 Squalene epoxidase (SQLE) promotes colorectal cancer (CRC) cell proliferation. (A) SQLE overexpression in LOVO and SW1116 cells promoted cell viability and (B) colony formation. (C) Knockdown of SQLE in HT29 and DLD1 cells significantly suppressed cell viability and (D) colony formation. (E) SQLE promotes tumour growth in vivo. SW1116 and LOVO cells (5×10^6 cells/tumour) transfected with SQLE or control vector were injected to nude mice aged 4 weeks. Tumour growth was significantly faster in SQLE overexpressing cells as compared with controls. (F) SQLE is overexpressed in two primary CRC organoids, and knockout of SQLE suppressed their growth. The significance of the difference between growth curves was determined by repeated-measures analysis of variance. Difference in colony formation was determined by two-tailed Student's t-test. *P<0.05; **p<0.01; ***p<0.001; ****p<0.0001. All experiments were conducted 3 times in triplicate.

oncogenic role of SQLE in CRC tumourigenesis. Histological examination by H&E staining confirmed CRC formation in the colon of Sqle tg mice, together with the increased proportion of mice with colon dysplasia and high-grade dysplasia (figure 4D). In concordance with these findings, the oncogenic function of SQLE in CRC was evidenced by increased cell proliferation evidenced by Ki-67 score (figure 4E) but decreased cell apoptosis by terminal deoxynucleotidyl transferase dUTP nick end labeling (TUNEL) score (figure 4F) in Sqle tg mice as compared with wild-type mice. To identify differentially expressed genes in Sqle tg mice, we performed Cancer Pathway PCR analysis of colon tissues from Sqle tg mice and their wild-type littermates. Cell cycle progression markers including Mki67, Ccnd2 and E2f4 are top upregulated genes, whereas pro-apoptotic genes Casp9 and Casp2 were downregulated, confirming the role of Sqle in promoting cell proliferation and suppressing apoptosis in CRC tumourigenesis (figure 4G).

SQLE knockout in mice suppressed colorectal tumourigenesis

Next, the effect of SQLE on CRC development was determined in CRISPR/Cas9-based whole body Sqle KO mice. We generated heterozygous Sqle mice (figure 4H), and performed the AOM-DSS chemical carcinogenesis model (figure 4I). As shown in figure 4I, Sqle KO mice showed decreased tumour number ($p<0.05$) in the colon as compared with wild-type littermates. Collectively, our findings in Sqle tg mice and Sqle KO mice both confirmed the oncogenic function of Sqle in colorectal tumourigenesis in vivo.

SQLE promotes de novo cholesterol biosynthesis

SQLE is the second rate-limiting enzyme for cholesterol biosynthesis. We hence evaluated its effect on cholesterol biosynthesis pathway. In LOVO and SW1116 cells, SQLE overexpression increased the mRNA expression of cholesterol biosynthesis genes (HMGCS1, HMGCR, MVK, PMVK, MVD, IDI1, FDPS and FDFT1) (online supplemental figure S2), whereas SQLE knockdown exerted an opposite effect (online supplemental figure S3). Western blot analysis demonstrated that SQLE overexpressing cells or Sqle tg mice have elevated HMGCR, FDFT1 and FDPS protein levels, while SQLE knockdown or $Sqle^{+/-}$ mice have downregulated protein levels of these genes (online supplemental figures S2 and S3). These data suggest that SQLE promotes

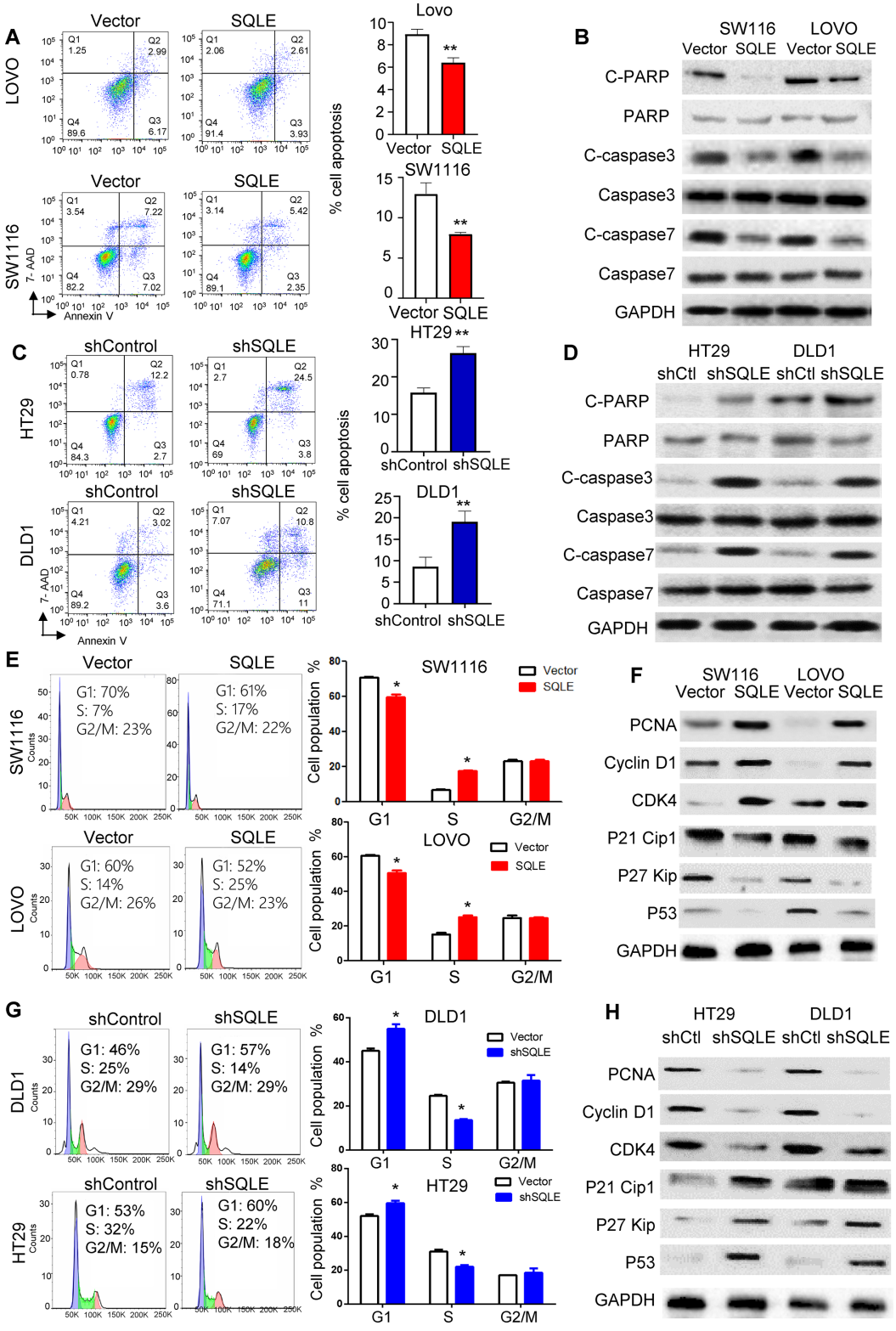

Figure 3 Squalene epoxidase (SQLE) suppresses cell apoptosis and promotes cell cycle progression in colorectal cancer (CRC) cells. (A) SQLE overexpression suppressed apoptosis in LOVO and SW1116 cells, as determined by annexin V/7-aminoactinomycin D (7-AAD) staining and flow cytometry analysis. (B) Western blot analysis indicated that SQLE overexpression suppressed the expression of cleaved PARP, caspase-3 and caspase-7. (C) Knockdown of SQLE in HT29 and DLD1 cells induced apoptosis by the annexin V/7-AAD assay. (D) SQLE knockdown increased cleaved PARP, caspase-3 and caspase-7 expression. (E) SQLE overexpression in LOVO and SW1116 cells led to a decrease of G_0/G_1 phase cell population concomitant with an increase of S phase cell population, as assessed by propidium iodide (PI) staining and flow cytometry. (F) SQLE overexpression enhanced the expression of PCNA, cyclin D1 and CDK4 that promotes G1 phase progression, while suppressing the expression of G1 gatekeepers $p21^{Cip1}$, $p27^{Kip1}$ and p53. (G) SQLE knockdown in HT29 and DLD1 cells led to accumulation of cells in G_0/G_1 phase with decreased S phase cell population. (H) SQLE silencing inhibited PCNA, cyclin D1 and CDK4, while inducing $p21^{Cip1}$, $p27^{Kip1}$ and p53 expression. The difference between two groups was determined by two-tailed Student's t-test. *P<0.05; **p<0.01. All experiments were conducted 3 times in triplicate.

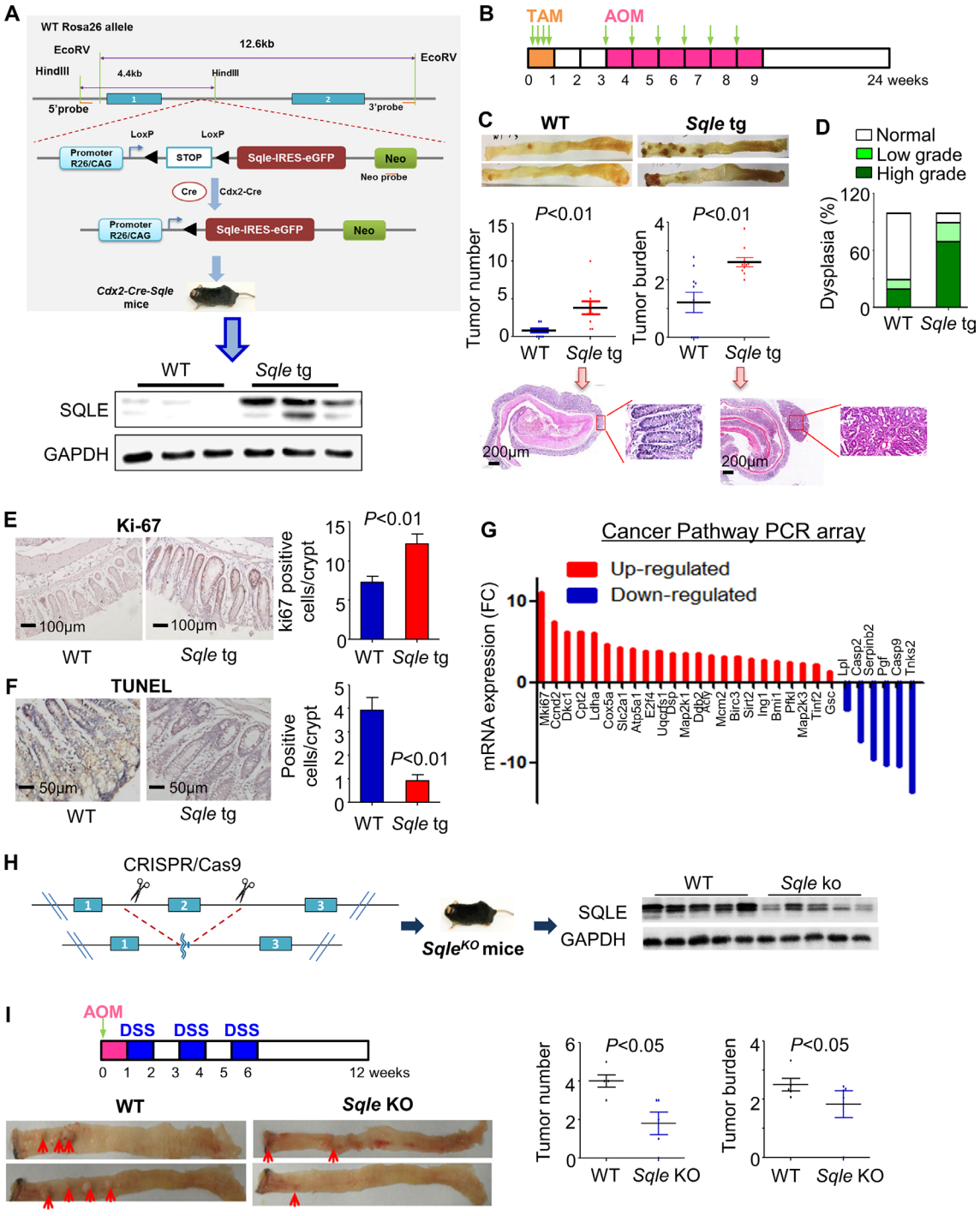

Figure 4 Colon-specific squalene epoxidase (Sqle) transgenic (tg) expression promotes colorectal tumourigenesis in mice. (A) The construction of colon-specific, conditional Sqle tg mice. Sqle transgene was introduced into the Rosa26 locus with Loxp sites flanking a STOP codon at 5′-end. These mice were then crossed to Cdx2-Cre^{ERT2} mice to obtain colon-specific Sqle tg mice. At 6 weeks of age, tamoxifen injection was given (100 mg/kg, intraperitoneally) for 4 times (one dose/day). Western blot analysis confirmed SQLE overexpression in colon tissues. (B) SQLE promotes chemically induced colorectal cancer (CRC). Sqle tg mice aged 6 weeks and wild-type (WT) littermates (n=10 per group) were injected with tamoxifen (100 mg/kg, intraperitoneally, 4 times), followed by azoxymethane (AOM) injection (10 mg/kg, intraperitoneally) for 6 times (once per week). Mice were sacrificed at week 24. (C) Colon-specific Sqle overexpression significantly increased the tumour number and burden in the colon (n=10 in each group). (D) Histological examination performed by a pathologist blinded to the nature of the samples confirmed that SQLE promoted tumour development, as the ratio of high grade of dysplasia in Sqle tg mice was 70%, while the corresponding ratio in WT mice was 20%. (E) Ki-67 staining showed that colon tissues of Sqle tg mice had higher cell proliferation as compared with WT mice. (F) TUNEL staining revealed that Sqle tg mice colon had reduced apoptosis as compared with WT mice. (G) Cancer Pathway PCR array analysis of colon tissues from Sqle tg and WT mice, which were first injected with tamoxifen (100 mg/kg, intraperitoneally, 4 times) and then sacrificed after 3 months. (H) The construction of CRISPR/Cas9-induced whole body Sqle knockout (KO) mice. Downregulation of SQLE in heterozygous Sqle KO mice colon was confirmed by western blot analysis. (I) Sqle KO mice and WT littermates were subjected to AOM-DSS regimen to induce CRC. Sqle KO mice developed significantly less colon tumours as compared with WT mice (n=5 in each group). The difference between two groups was determined by two-tailed Student's t-test.

de novo cholesterol biosynthesis pathway, which contributes to increased cell proliferation in CRC cells.

Sqle transgenic mice displayed gut dysbiosis

Besides CRC cell intrinsic effects of SQLE, we asked if SQLE have an impact on the colonic microenvironment. Gut microbiota dysbiosis is an emerging aetiological factor in colorectal tumourigenesis.[19] We therefore asked if gut dysbiosis, at least in part, mediates the oncogenic effect of Sqle in vivo. Shotgun metagenome analysis was performed on stools collected from Sqle tg and wild-type mice at 3 months of age. Beta-diversity analysis did not show separate clusters for Sqle tg mice versus wild-type mice (figure 5A), while the alpha diversity index revealed a decreased trend in Sqle tg ($p=0.093$) (figure 5A). We determined alterations in the bacterial composition of Sqle tg and wild-type mice at the species level, and unravelled outlier bacterial species with significant differential abundance among the two groups (fold change >2; $p<0.05$) (figure 5B). Interestingly, we observed significant enrichment of pathogenic bacterial species such as *Desulfovibrio fairfieldensis*, *Rhodococcus erythropolis*, *Brucella abortus* and *Chlamydia muridarum* were enriched in Sqle tg mice, while protective bacteria were depleted, including *Streptomyces violaceusniger* and *Pseudomonas* sp *Leaf58* (figure 5C). The changes in these key bacterial species were confirmed by qPCR (figure 5D). These results suggest that Sqle overexpression in vivo promotes gut dysbiosis.

Sqle transgenic mice showed altered gut metabolomics

Since some of the enriched pathogenic bacterial species are known to possess various metabolic activities, we next performed non-targeted metabolomic profiling on the same stool samples. Principal component analysis showed that the metabolome of the Sqle tg can be separated from that of wild-type mice (figure 5E). Focusing on differentially abundant metabolites (figure 5F,G), we found that secondary bile acids, such as lithocholic acid, chenodeoxycholic acid, taurodeoxycholic acid and deoxycholic acid were enriched in the stools from Sqle tg mice as compared with wild-type mice (figure 5G). Increased levels of secondary bile acids including lithocholic acid, isolithocholic acid, isoallolithocholic acid and deoxycholic acid in the Sqle tg mice were validated by targeted metabolomic analysis (figure 5H).

As secondary bile acids are bio-transformed from primary bile acids via the action of gut microbiome,[20] we investigated the correlation between gut bacterial species and metabolites showing differential abundances in Sqle tg mice (figure 6A). We observed the significant correlations between secondary bile acids and *C. muridarum*, implying its potential involvement in contributing to increased secondary bile acids. Moreover, all four pathogenic bacteria showed positive association with key altered metabolites (figure 6A). Sqle transgene expression thus modulates the gut microbiome and metabolites in CRC development in mice.

SQLE transgenic overexpression impairs the intestinal barrier function and promotes inflammation

Secondary bile acids are known lipotoxins, whose increased levels is an important risk factor for CRC.[21] They are toxic to colonic epithelial cells and are known to disrupt the gut barrier function.[22] Gut microbial dysbiosis is also closely associated with the disruption of the gut barrier.[23] We therefore compared the barrier function of Sqle tg mice and wild-type littermates by FITC-dextran transepithelial permeability assay. After oral gavage of FITC-dextran, higher serum FITC-dextran was detected in Sqle tg mice as compared with wild-type mice (figure 6B). Electron microscopy (EM) confirmed the disruption of tight junctions in Sqle tg mice (figure 6C). Epithelial tight junctions are maintained by intercellular junctional protein complexes. We determined expression of key tight junction proteins by western blot analysis, and revealed that Jam-c and occludin were downregulated in the Sqle tg mice colon as compared with that of wild-type mice (figure 6D). Moreover, Muc2, a key component of inner mucus, was downregulated at mRNA level in Sqle tg mice (figure 6E). A major consequence of a 'leaky' gut is the induction of a pro-inflammatory response. In line with this notion, inflammatory pathway PCR array analysis of Sqle tg colon tissues showed the significant upregulation of pro-inflammatory factors such as Cxcl3, Crp and Cxcr2 (online supplemental figure S4). These findings indicate the gut dysbiosis-metabolite axis might contribute to gut barrier dysfunction in Sqle tg mice.

SQLE overexpression-induced gut microbiota dysbiosis promotes gut barrier dysfunction and colonic epithelium proliferation in germ-free mice

To address whether Sqle tg expression-induced gut dysbiosis has a direct effect on colon cell proliferation, stools collected from Sqle tg mice and wild-type mice from the AOM model was transplanted to germ-free (GF) mice. One month later, mice were sacrificed. The oral gavage of different stools had no impact on body weight. Prior to sacrifice, we performed FITC-dextran transepithelial permeability assay, showing that FITC-dextran in the serum of GF mice gavaged with stool of Sqle tg mice was significantly higher than those gavaged with stool of wild-type mice (figure 6F) and disruption of gut barrier was confirmed by EM (figure 6G). Consistently, junction adhesion protein Jam-c and occludin were downregulated in GF mice gavaged with Sqle tg stool compared with wild-type stool (figure 6H). Moreover, Ki-67 staining demonstrated that Sqle tg mice stool significantly promoted proliferation of colonic epithelial cells of GF mice compared with wild-type mice stool (figure 6I). These data underscore a functional role of SQLE-induced gut microbiota dysbiosis in impairing gut barrier function and promoting colonic cell growth.

Pharmacological inhibition of Sqle improves therapeutic efficacy of chemotherapy in CRC treatment

Given that SQLE possesses oncogenic function in CRC, we next investigated if SQLE can be therapeutically targeted in CRC cells. To test whether SQLE represents a viable therapeutic target for CRC, we treated HT29 and DLD1 cells with terbinafine, an FDA-approved fungal SQLE inhibitor. As shown in figure 7A, terbinafine dose-dependently suppressed the growth of HT29 and DLD1 cells in vitro. Apart from CRC cell lines, terbinafine significantly impaired the growth of primary CRC organoids (figure 7A). We next assessed the effect of terbinafine in combination with oxaliplatin or 5-FU, the common chemotherapeutic drugs used for the treatment of patients with CRC. We performed cell viability assay in the presence or absence of terbinafine, which showed that terbinafine sensitised HT29 and DLD1 cells to the growth inhibitory effects of both oxaliplatin and 5-FU (figure 7B). Quantitative assessment using combination index (CI) demonstrated that combination of terbinafine with oxaliplatin (CI: 0.39–0.63) or 5-FU (CI: 0.332–0.472) was synergistic (<1) (figure 7C). In addition, apoptosis assay showed that the combination of terbinafine with oxaliplatin and 5-FU synergistically induced apoptosis in vitro (figure 7D). Terbinafine

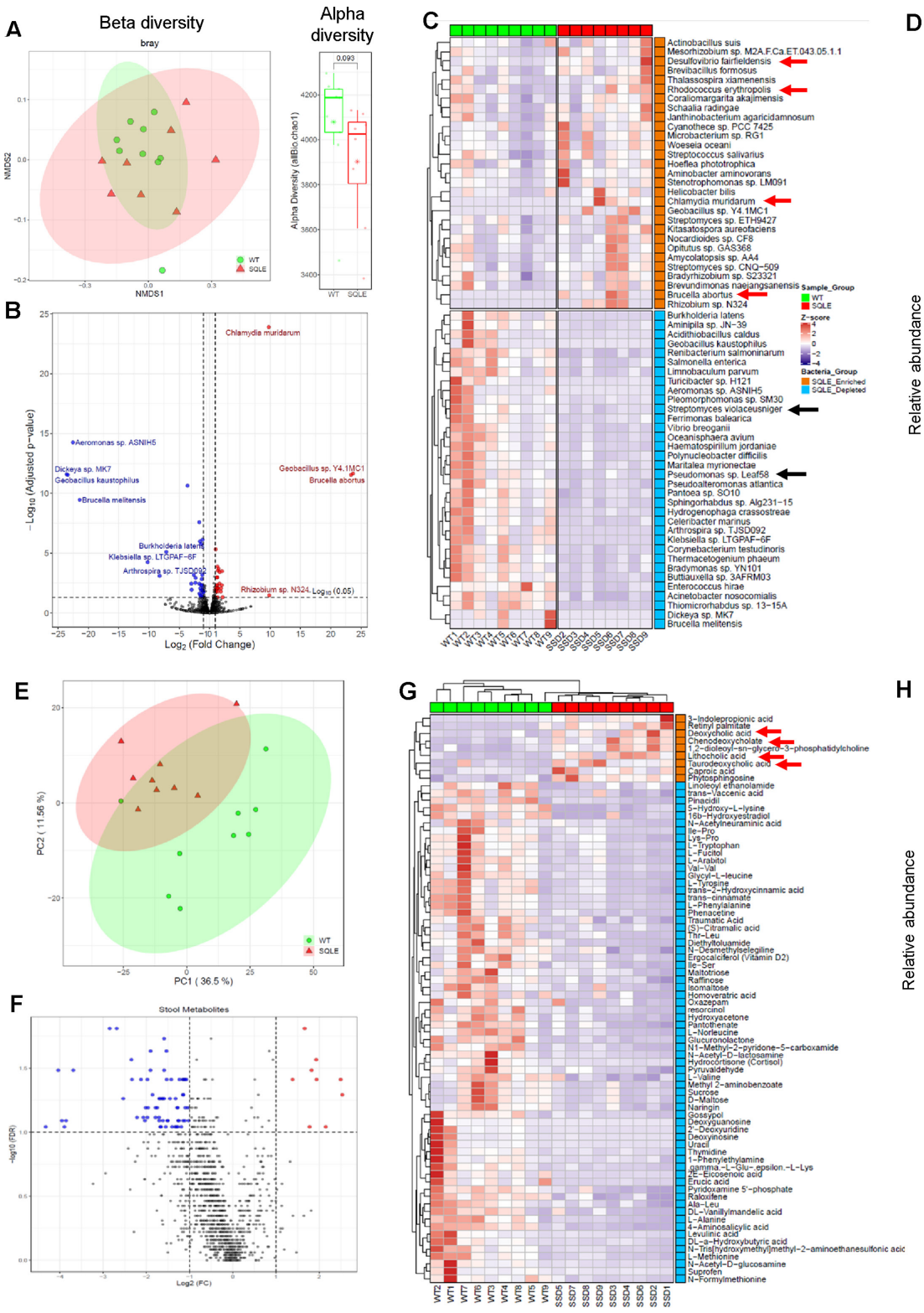

Figure 5 Colon-specific squalene epoxidase (Sqle) transgenic (tg) expression in mice dysregulate gut microbiota and metabolites. (A) Metagenomic sequencing was performed on stool obtained from Sqle tg mice and wild-type (WT) littermates at 3 months after tamoxifen injection. Principal component analysis (PCA) of bacteria composition between Sqle tg (n=8) and WT (n=9) mice (left). Alpha-diversity showed a decreasing trend in Sqle tg mice (right). (B and C) Volcano plot and heat map analysis revealed 29 enriched bacteria, including pathogenic bacteria, *Desulfovibrio fairfieldensis*, *Rhodococcus erythropolis*, *Brucella abortus* and *Chlamydia muridarum*, and 34 depleted bacteria such as *Streptomyces violaceoruber*, *Pseudomonas* sp *Leaf58* in Sqle tg mice. (D) Quantitative PCR (qPCR) validation of key bacterial species altered in Sqle tg mice. (E) Global metabolomics profiling was performed on stool samples from Sqle tg mice and WT littermates at 3 months of age. PCA analysis of metabolite profiles (n=9 for each group). (F and G) Volcano plot and heat map analysis revealed nine enriched metabolites such as deoxycholic acid (DCA), lithocholic acid (LCA), taurodeoxycholic acid (TDCA) and chenodeoxycholic acid (CDCA); plus 64 depleted metabolites in Sqle tg mice as compared with WT littermates. (H) Targeted metabolomic analysis of secondary bile acids by liquid chromatography-mass spectrometry. *P<0.05; **p<0.01.

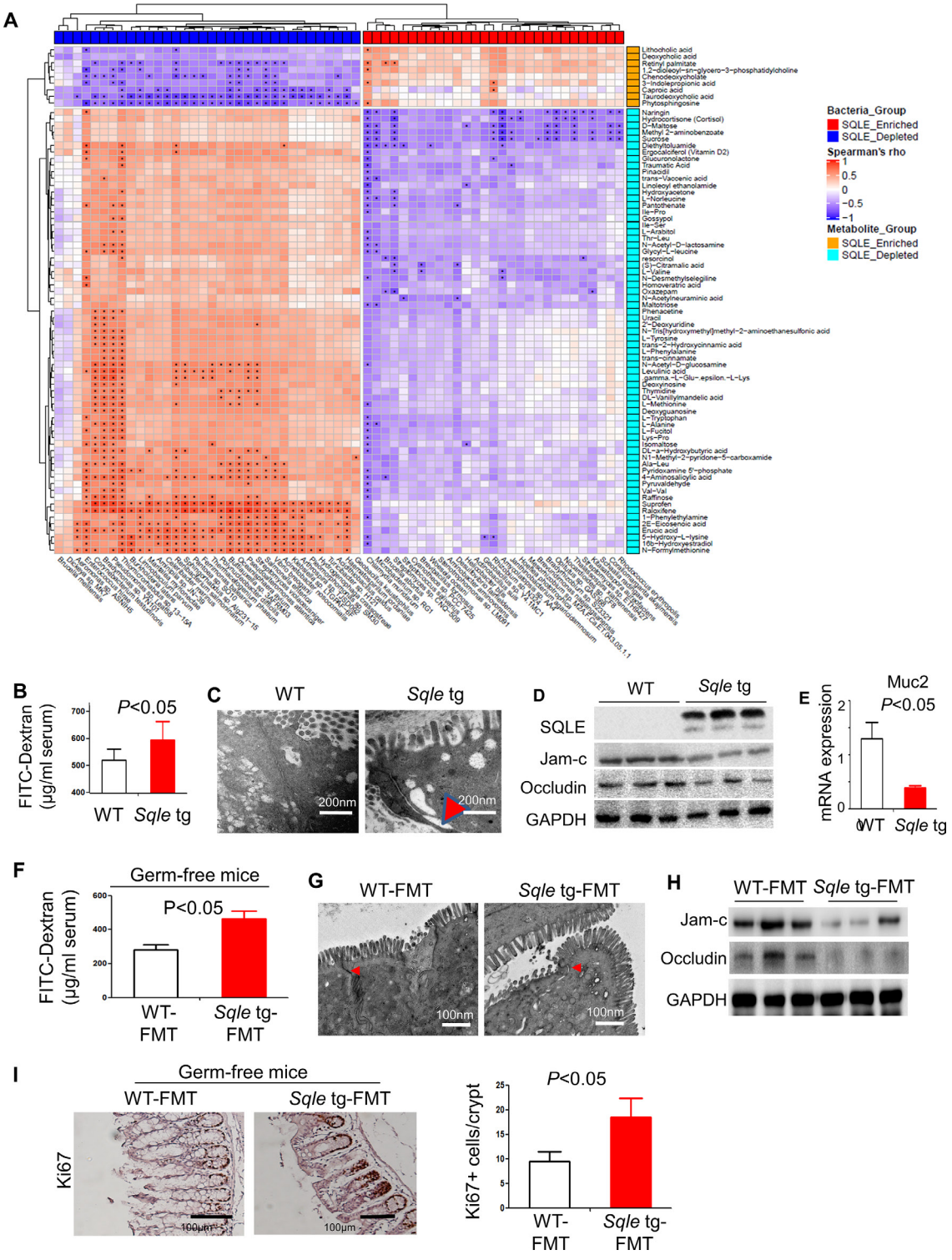

Figure 6 Gut microbiota-metabolite axis contributes to gut barrier dysfunction in squalene epoxidase (Sqle) transgenic (tg) mice and in germ-free mice receiving faecal microbiota transplantation (FMT) from Sqle tg mice. (A) Correlation analysis revealed that pathogenic bacteria are positively correlated with altered metabolites, including secondary bile acids. (B) Fluorescein isothiocyanate (FITC)-dextran intestinal permeability test was performed on Sqle tg mice and wild-type (WT) littermates at 3 months after tamoxifen injection, revealing that the gut barrier was impaired in Sqle tg mice. (C) Electron microscopy confirmed impaired intestinal tight junction in Sqle tg mice. (D) Western blot analysis showed that tight junction proteins Jam-c and occludin were downregulated in Sqle tg mice. (E) Muc2 messenger RNA (mRNA) was downregulated in Sqle tg mice. (F) Stool collected from Sqle tg and WT littermates was gavaged to germ-free mice aged 6 weeks. One month later, FITC-dextran was gavaged 4 hours before sacrifice to perform permeability assay. Intestinal permeability was significantly induced in germ-free mice gavaged with stool from Sqle tg mice. (G) Electron microscopy confirmed the impaired intestinal tight junction germ-free mice fed with stool from Sqle tg mice. (H) Western blot analysis showed that tight junction proteins Jam-c and occludin were downregulated in germ-free mice gavaged with stool from Sqle tg mice. (I) Germ-free mice transplanted with Sqle tg mice stool showed increased Ki-67 staining in the colon epithelium as compared with those gavaged with WT mice stool. Two-tailed Student's t-test was used for the difference determination between two groups.

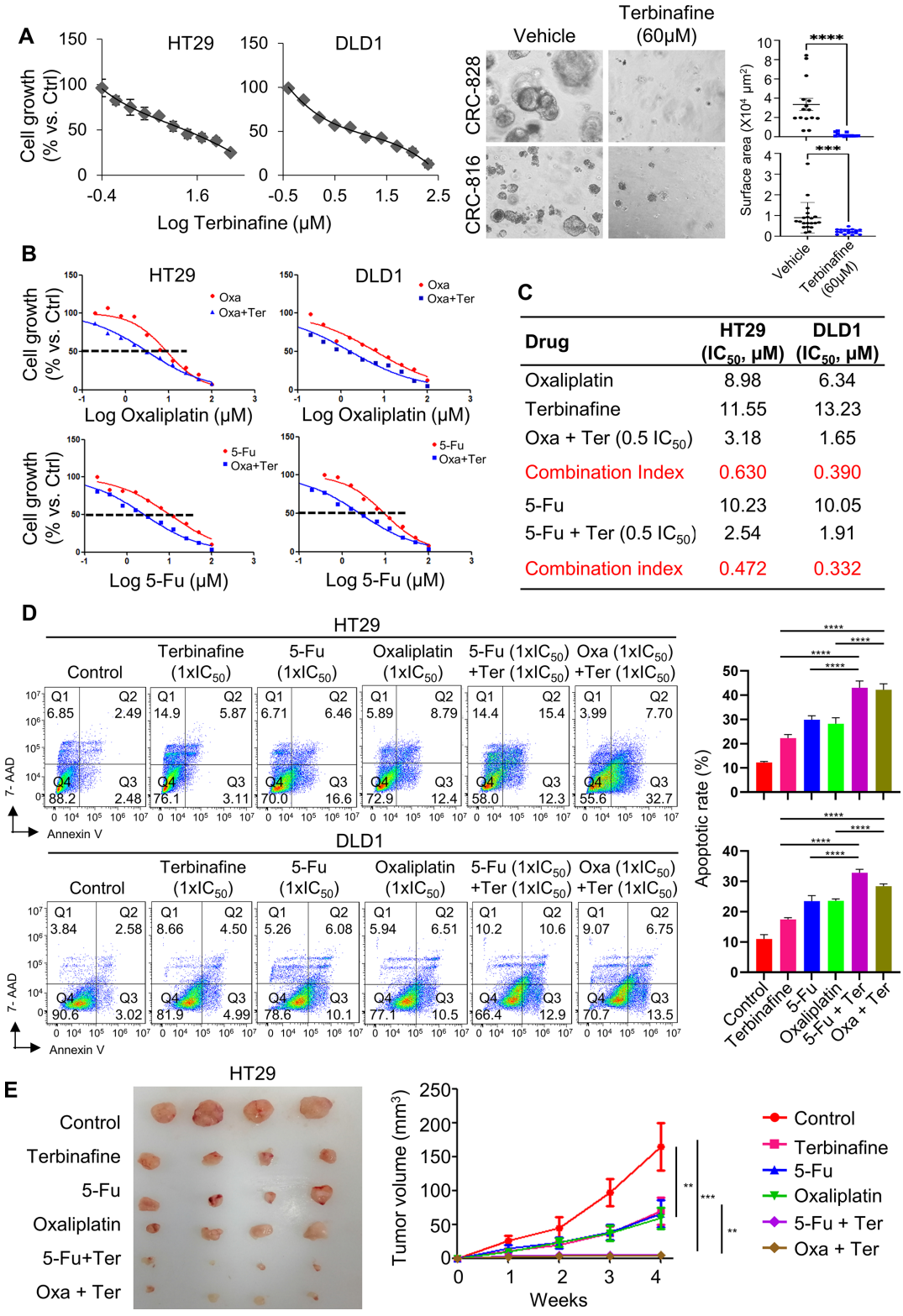

Figure 7 Squalene epoxidase (SQLE) is a therapeutic target in colorectal cancer (CRC). (A) Terbinafine, a Food and Drug Administration-approved drug targeting SQLE, dose-dependently suppressed cell viability of HT29 and DLD1 cells, and primary CRC organoids. (B) Terbinafine co-treatment sensitised HT29 and DLD1 cells to the growth inhibitory effect of 5-fluorouracil (5-FU) or oxaliplatin. (C) Combination index (CI) indicated that terbinafine+5-FU or oxaliplatin exerted synergistic effects for the treatment of CRC cells, with CI <1. (D) Apoptosis assay showed that terbinafine+5-FU or oxaliplatin (48 hours) synergistically induced apoptosis in CRC cells. (E) Nude mice were injected subcutaneously with HT29 cells, randomised and then treated with (1) vehicle, (2) terbinafine (80 mg/kg, oral daily), (3) 5-FU (30 mg/mg, intraperitoneally, once per week), (4) oxaliplatin (10 mg/kg, intraperitoneally, twice per week), (5) terbinafine+5-FU and (6) terbinafine+oxaliplatin. Terbinafine treatment alone suppressed tumour growth significantly by ~50%. On the other hand, terbinafine combined with 5-FU or oxaliplatin showed synergistic effects in suppressing tumour size in nude mice as compared with 5-FU or oxaliplatin single treatments. The significance of the difference between tumour growth rate was determined by repeated-measures analysis of variance. **p<0.01; ***p<0.001; ****p<0.0001. All in vitro experiments were conducted 3 times in triplicate.

also potentiated 5-FU-induced cell cycle arrest (online supplemental figure S5).

To confirm the synergistic effect of terbinafine plus 5-FU or oxaliplatin in suppressing CRC growth, we performed subcutaneous xenograft model in nude mice. HT29 cells (1×10^6) were implanted into the dorsal flanks of nude mice, and divided into six groups: (1) vehicle; (2) terbinafine; (3) 5-FU; (4) oxaliplatin; (5) terbinafine+5-FU and (6) terbinafine+oxaliplatin. As shown in figure 7E, single drug treatments inhibited tumour growth by approximately 50% ($p<0.01$). Importantly, either the combination of terbinafine+5-FU or terbinafine+oxaliplatin triggered complete growth arrest ($p<0.001$) as compared with vehicle and was significantly more effective than single drug treatments ($p<0.01$). Our data indicate that SQLE is an actionable target in CRC and that SQLE inhibition could improve the therapeutic efficacy of chemotherapy in CRC.

DISCUSSION

In this study, we established SQLE as an oncogenic factor in CRC using cell lines, colon-specific Sqle tg mice and Sqle KO mice models. We revealed that SQLE mediates tumourigenesis via both cell intrinsic effects and the modulation of gut microbiota-metabolite axis, which respectively drives tumour cell proliferation and intestinal barrier dysfunction. We further demonstrated that SQLE inhibitor, terbinafine, could be re-purposed for the treatment of CRC by exerting synergistic effects in combination with chemotherapy. Corroborating our preclinical findings, SQLE is overexpressed in CRC and its expression predicts poor patient survival, implying SQLE as a therapeutic target and prognosification factor in CRC.

Our work clearly demonstrated that SQLE functions as a tumour cell-intrinsic oncogenic factor in CRC. Ectopic expression of SQLE in CRC cells promoted cell proliferation by accelerating cell cycle progression and suppressed cell apoptosis, whereas KO of SQLE exerted opposite effects. To validate the effect of SQLE in vivo, we established colon-specific Sqle tg mice and $Sqle^{+/-}$ mice to comprehensively evaluate the effect of Sqle gain-of-function and loss-of-function in colorectal carcinogenesis. Consistent with our notion that SQLE is an oncogene, colon-specific Sqle overexpression exacerbated AOM-induced CRC, both in terms of tumour incidence and disease severity, and tumours from Sqle tg mice exhibited significantly higher cell proliferation indices. In contrast, Sqle KO impaired AOM-DSS-induced CRC. The pro-tumourigenic effect of SQLE could be partly attributed to induction of cholesterol biosynthesis, which is critical for supporting increased cell proliferation. All these findings collectively show that SQLE functions as an oncogene in CRC tumourigenesis.

Accumulating evidence suggests that colorectal tumourigenesis involved a complex interaction of tumour cells and its microenvironment.[24] In particular, the gut microbiota is increasingly recognised as causative agents for CRC. Previously, we have shown that GF mice orally gavaged with stools from patients with CRC had significantly induced colonic cell proliferation and tumourigenesis.[19] However, it is unclear if the interplay between genetic alterations and gut dysbiosis plays a role in colorectal tumourigenesis. Here, we demonstrated that Sqle transgene expression in mice induces gut dysbiosis, characterised by the enrichment of several pathogenic bacteria including *D. fairfieldensis*, *R. erythropolis*, *B. abortus* and *C. muridarum*, that are associated with various pathologies[25–27]; while potential protective bacteria with anti-inflammatory and antitumour properties, *S. violaceusniger* and *Pseudomonas* sp *Leaf58*, were depleted.[28–30] Transplantation of Sqle tg stool to GF mice significantly promoted the proliferation of the colonic epithelial cells as compared with wild-type mice, implying that Sqle-induced gut dysbiosis plays a casual role in CRC. These data imply that Sqle impacts the gut microbiome beyond its direct effect on tumour cell proliferation and survival.

Studies have shown that metabolites and microbiota can affect each other reciprocally in gut.[31] Metabolomic profiling marked the induction of secondary bile acids in the stool of Sqle tg mice. Since secondary bile acids are products of microbial metabolism, we integratively analysed metagenome and metabolome datasets. Indeed, we identified that secondary bile acids positively correlated with *C. muridarum*, an outlier pathogenic bacteria in Sqle tg mice. Secondary bile acids are important lipotoxins that are known to induce DNA damage in colonic epithelium[32] and promote colon cancer formation in mice.[33] Consistent with this, we found that gut barrier function was impaired in Sqle tg mice, as shown by increased intestinal permeability, EM analysis and downregulation of tight junction proteins. Accompanying the compromised gut barrier integrity is an inflammatory response in Sqle tg mice, which further exacerbated colorectal tumourigenesis. These results indicate the gut dysbiosis-metabolite-gut barrier axis might contribute, at least in part, to the tumour promoting effect of SQLE in vivo.

Given the important role of SQLE in CRC development, we next evaluated its potential as a therapeutic target. We thus tested terbinafine, an FDA-approved drug for antifungal infection, as a novel treatment for CRC. In line with the oncogenic function of SQLE, its blockade by terbinafine exerted growth inhibitory effects on CRC cells. In particular, terbinafine in combination with 5-FU or oxaliplatin, chemotherapy commonly used in CRC, synergistically suppressed CRC growth in vitro and in vivo. Our results suggest that the re-purposing of terbinafine might be a strategy for the treatment of CRC in combination with chemotherapy.

Corroborating our experimental results, analysis of independent human CRC cohorts revealed that SQLE is overexpressed in CRC and its expression predicts poor survival in patients with CRC. In agreement with our data, Kim *et al* and He *et al* both reported that SQLE protein expression predicts poor survival of patients with CRC.[10 11] On the contrary, Jun *et al* demonstrated that high SQLE predicts favourable outcomes specifically in patients with stage IV CRC, and that depletion of SQLE promotes metastasis phenotypes in CRC cells. SQLE may thus have disparate effects on CRC growth and metastasis. Studies on the role of SQLE in CRC metastasis using Sqle transgenic or KO mice are warranted in the future.

In conclusion, our work establishes an oncogenic role of SQLE in CRC. SQLE promotes CRC cell proliferation and survival, and exerts an influence on the tumour microenvironment by causing gut microbiota and gut barrier dysfunction. Targeting of SQLE by terbinafine significantly improved the efficacy of conventional chemotherapy, indicating its potential clinical application in CRC treatment in the future.

Author affiliations
[1]Institute of Digestive Disease and The Department of Medicine and Therapeutics, State Key Laboratory of Digestive Disease, Li Ka Shing Institute of Health Sciences, CUHK Shenzhen Research Institute, The Chinese University of Hong Kong, Hong Kong SAR, China
[2]Department of Laboratory Animal Science, College of Basic Medical Sciences, Army Medical University, Chongqing, China
[3]Department of Anatomical and Cellular Pathology, State Key Laboratory of Translational Oncology, The Chinese University of Hong Kong, Hong Kong SAR, China
[4]Lee Kong Chian School of Medicine, Nanyang Technological University, Singapore

Correction notice This article has been corrected since it published Online First. Online supplemental file 1 has been replaced. Human SQLE qPCR primers in Table S4 are corrected as follow: Human SQLE qPCR Forward: 5′-GATGATGCAGCTATTT TCGAGGC-3′; Reverse: 5′-CCTGAGCAAGGATATTCACGACA-3.

Contributors Chuangen Li (CL) performed the experiments, analysed the data and drafted the manuscript; YW provided the facilities for the animal work; DL and YZ provided the transgenic mouse model and commented on the study; CCW commented on the study and revised manuscript; OOC and Changan Liu (CL) performed bioinformatics analyses; YL performed the organoid experiments; XZ and JJYS commented on the study; WK and KFT assisted for tissue microarray; JY designed, supervised the project and revised the manuscript. JY is the guarantor for this paper.

Funding This project was supported by National Key R&D Programme of China (No. 2020YFA0509200/2020YFA0509203), National Natural Science Foundation of China (NSFC; 81972576), RGC-CRF Hong Kong (C4039-19GF and C7065-18GF), RGC-GRF Hong Kong (14110819, 24100520 and 14108718), Health and Medical Research Fund (06170686 and 07181256) and Vice-Chancellor's Discretionary Fund CUHK.

Competing interests None declared.

Patient consent for publication Not applicable.

Ethics approval This study involves human participants and was approved by Human Ethics Committee of Beijing University Cancer Hospital and the Chinese University of Hong Kong (ID: CREC Ref. 2019.425). Participants gave informed consent to participate in the study before taking part. All animal studies were performed in accordance with guidelines approved by the Animal Experimentation Ethics Committee of the Chinese University of Hong Kong (AMUWEC-20192185).

Provenance and peer review Not commissioned; externally peer reviewed.

Data availability statement Data are available on reasonable request. All data are available from the corresponding author on request.

ORCID iDs
Wei Kang http://orcid.org/0000-0002-4651-677X
Joseph JY Sung http://orcid.org/0000-0003-3125-5199
Jun Yu http://orcid.org/0000-0001-5008-2153

REFERENCES

1 Liu P-H, Wu K, Ng K, *et al*. Association of obesity with risk of early-onset colorectal cancer among women. *JAMA Oncol* 2019;5:37–44.
2 Yang MH, Rampal S, Sung J, *et al*. The association of serum lipids with colorectal adenomas. *Am J Gastroenterol* 2013;108:833–41.
3 Yang J, Yu J. The association of diet, gut microbiota and colorectal cancer: what we eat may imply what we get. *Protein Cell* 2018;9:474–87.
4 Beyaz S, Mana MD, Roper J, *et al*. High-Fat diet enhances stemness and tumorigenicity of intestinal progenitors. *Nature* 2016;531:53–8.
5 Ecker J, Benedetti E, Kindt ASD, *et al*. The colorectal cancer lipidome: identification of a robust tumor-specific lipid species signature. *Gastroenterology*. In Press 2021;161:910–23.
6 Ogino S, Nosho K, Meyerhardt JA, *et al*. Cohort study of fatty acid synthase expression and patient survival in colon cancer. *JCO* 2008;26:5713–20.
7 Tsoi H, Chu ESH, Zhang X, *et al*. Peptostreptococcus anaerobius induces intracellular cholesterol biosynthesis in colon cells to induce proliferation and causes dysplasia in mice. *Gastroenterology* 2017;152:1419–33.
8 Jun SY, Brown AJ, Chua NK, *et al*. Reduction of squalene epoxidase by cholesterol accumulation accelerates colorectal cancer progression and metastasis. *Gastroenterology* 2021;160:1194–207.
9 Jia W, Xie G, Jia W. Bile acid–microbiota crosstalk in gastrointestinal inflammation and carcinogenesis. *Nat Rev Gastroenterol Hepatol* 2018;15:111–28.
10 He L, Li H, Pan C, *et al*. Squalene epoxidase promotes colorectal cancer cell proliferation through accumulating calcitriol and activating CYP24A1-mediated MAPK signaling. *Cancer Commun* 2021;41:726–46.
11 Kim JH, Kim CN, Kang DW. Squalene epoxidase correlates E-cadherin expression and overall survival in colorectal cancer patients: the impact on prognosis and correlation to clinicopathologic features. *J Clin Med* 2019;8:632.
12 Liu D, Wong CC, Fu L, *et al*. Squalene epoxidase drives NAFLD-induced hepatocellular carcinoma and is a pharmaceutical target. *Sci Transl Med* 2018;10:eaap9840.
13 Li H, Durbin R. Fast and accurate long-read alignment with Burrows–Wheeler transform. *Bioinformatics* 2010;26:589–95.
14 Li H, Handsaker B, Wysoker A, *et al*. The sequence Alignment/Map format and SAMtools. *Bioinformatics* 2009;25:2078–9.
15 Wood DE, Lu J, Langmead B. Improved metagenomic analysis with Kraken 2. *Genome Biol* 2019;20:257.
16 Faccin TC, Masuda EK, Piazer JVM, *et al*. Annular Stenotic Oesophageal Squamous Cell Carcinoma in Cattle Exposed Naturally to Bracken Fern (Pteridium arachnoideum). *J Comp Pathol* 2017;157:174–80.
17 Love MI, Huber W, Anders S. Moderated estimation of fold change and dispersion for RNA-Seq data with DESeq2. *Genome Biol* 2014;15:550.
18 McMurdie PJ, Holmes S. phyloseq: an R package for reproducible interactive analysis and graphics of microbiome census data. *PLoS One* 2013;8:e61217.
19 Wong SH, Zhao L, Zhang X, *et al*. Gavage of Fecal Samples From Patients With Colorectal Cancer Promotes Intestinal Carcinogenesis in Germ-Free and Conventional Mice. *Gastroenterology* 2017;153:1621–33.
20 Louis P, Hold GL, Flint HJ. The gut microbiota, bacterial metabolites and colorectal cancer. *Nat Rev Microbiol* 2014;12:661–72.
21 Debruyne PR, Bruyneel EA, Li X, *et al*. The role of bile acids in carcinogenesis. *Mutat Res* 2001;480-481:359–69.
22 Cao H, Xu M, Dong W, *et al*. Secondary bile acid-induced dysbiosis promotes intestinal carcinogenesis. *Int. J. Cancer* 2017;140:2545–56.
23 Martinez-Medina M, Denizot J, Dreux N, *et al*. Western diet induces dysbiosis with increased *E coli* in CEABAC10 mice, alters host barrier function favouring AIEC colonisation. *Gut* 2014;63:116–24.
24 Angell HK, Bruni D, Barrett JC, *et al*. The immunoscore: colon cancer and beyond. *Clin Cancer Res* 2020;26:332–9.
25 Goldstein EJC, Citron DM, Peraino VA, *et al*. *Desulfovibrio desulfuricans* Bacteremia and Review of Human *Desulfovibrio* Infections. *J Clin Microbiol* 2003;41:2752–4.
26 Rungue M, Melo V, Martins D, *et al*. NLRP6-associated host microbiota composition impacts in the intestinal barrier to systemic dissemination of Brucella abortus. *PLoS Negl Trop Dis* 2021;15:e0009171.
27 Howe SE, Shillova N, Konjufca V. Dissemination of Chlamydia from the reproductive tract to the gastro-intestinal tract occurs in stages and relies on Chlamydia transport by host cells. *PLoS Pathog* 2019;15:e1008207.
28 Hayakawa M, Yoshida Y, Iimura Y. Selective isolation of bioactive soil actinomycetes belonging to the Streptomyces violaceusniger phenotypic cluster. *J Appl Microbiol* 2004;96:973–81.
29 Ma J, Cao B, Chen X, *et al*. Violacin a, a new chromanone produced by Streptomyces violaceoruber and its anti-inflammatory activity. *Bioorg Med Chem Lett* 2018;28:947–51.
30 Helfrich EJN, Vogel CM, Ueoka R, *et al*. Bipartite interactions, antibiotic production and biosynthetic potential of the Arabidopsis leaf microbiome. *Nat Microbiol* 2018;3:909–19.
31 Peng Y, Nie Y, Yu J, *et al*. Microbial metabolites in colorectal cancer: basic and clinical implications. *Metabolites* 2021;11:159.
32 Booth LA, Gilmore IT, Bilton RF. Secondary bile acid induced DNA damage in HT29 cells: are free radicals involved? *Free Radic Res* 1997;26:135–44.
33 Bernstein C, Holubec H, Bhattacharyya AK, *et al*. Carcinogenicity of deoxycholate, a secondary bile acid. *Arch Toxicol* 2011;85:863–71.

Supplementary Methods

Human CRC cancer cell lines

SW1116, LOVO, HT29 and DLD1 cells were purchased from the American Type Culture Collection (ATCC, Manassas, VA) and grown in DMEM supplemented with 10% fetal bovine serum (FBS) and antibiotics. All cell lines were cultured at 37°C in an incubator with 95% air and 5% CO_2 supply.

RNA extraction, semi-quantitative RT-PCR, and real-time PCR analyses

Total RNA was extracted from cells and tissues using TRIzol^{TM}. cDNA was synthesized from 1μg of total RNA using Transcriptor Reverse Transcriptase (Roche). Real-time PCR was performed using SYBR Green master mix (Roche) on LightCycler 480. Each sample was performed in triplicate. ΔΔCT method was applied to determine the fold change in gene expression. Primer sequences are listed in **Table S4**.

Plasmids and gene transfection

pCMV-SQLE (RC202008), pCMV control plasmids, SQLE shRNA (TL309122V), and control shRNA (pGFP-C-shLenti) plasmids were ordered from OriGene. pCMV control and pCMV-SQLE plasmids were transfected into CRC cells using Lipofectamine 2000 (Invitrogen). For stable cell lines selection, cells were passed into fresh growth medium with 800mg/ml neomycin (G418). After one month of selection, cells were harvested to detect SQLE expression. For shRNA, lentivirus was generated using HEK293T cells by transfection of shRNA plasmid with packaging plasmids. After 72h post-transfection,

the culture supernatants were used for transduction of CRC cells. For stable cell lines selection, cells were passed into fresh growth medium with 2μg/ml puromycin. After 2 weeks of selection, cells were harvested to detect SQLE expression.

Western blot

20-40 mg protein was loaded onto 12% SDS-PAGE and transferred to an equilibrated polyvinylidenedifluoride (PVDF) membrane (Invitrogen). After blocking in 5% BSA dissolved in TBST solution at room temperature for 1h, the membrane was incubated with primary antibody in 5% BSA overnight at 4°C. After washing steps, the membrane was incubated with secondary antibody for 1h at room temperature. After 4 washing steps, protein was detected by enhanced chemiluminescence reagent (ECL, Amersham Corporation, Heights, IL, USA). Antibodies used in this study are shown in **Table S5**.

Colony formation assay

For the cell colony formation assay, stably transfected cells (1000/well) were plated in 6-well plates. After culturing for 7 days, cells were fixed with 70% ethanol and stained with 0.25% crystal violet solution. Colonies with over 50 cells per colony were counted. All experiments were conducted three times in triplicate.

Transmission Electron Microscopy

Small pieces of colon tissues (1mm^3) from germ-free mice (fed with stools from Sqle tg mice or wildtype mice) were collected and fixed in 2.0% glutaraldehyde in 0.1 mol/L

sodium cacodylate (Electron Microscopy Sciences, Hatfield, PA). The ultrathin sections were prepared on a Reichert Ultracut E ultramicrotome, and examined using a Philips CM100 transmission electron microscope.

Microbial DNA Extraction and Bacteria Quantification

DNA was extracted from mice stools using the DNeasy PowerSoil Kit (QIAGEN) according to the manufacturer's instructions. For qPCR quantification of differentially expressed bacteria, genomic DNA was amplified by qPCR with universal SYBR Green PCR Master Mix (Takara) on the ABI QuantStudio 7 Flex Real-Time PCR System, and normalized to 16S gene abundance. Primers used for detecting specific bacteria species are listed in **Table S6**. For *Desulfovibrio Fairfieldensis*, *Rhodococcus erythropolis*, *Chlamydia muridarum*, *Streptomyces violaceusniger*, *Pseudomonas sp.* Leaf58, primer was designed using NCBI/Genebank. When target Genebank sequences were chosen, "pick primers" was applied (nr database and Bacteria organism). Specificity of primers was examined using NCBI/Primer-Blast to confirm that no off-target bacteria could be amplified by the primers. Genebank numbers and targeted proteins were listed in **Table S6**. For *Brucella abortus*, the primer sequences were reported previously [1] and its specificity was confirmed using NCBI/Primer-Blast.

Patient-derived CRC organoids

Primary CRC organoids (CRC-816, CRC-828) were obtained from Princess Margaret Living Biobank (Canada), and cultured in DMEM/F12 with N2 and B27 supplements

(ThermoFisher), 10mmol/L HEPES, 1.25mmol/L N-acetyl cysteine (Sigma-Aldrich, St Louis, MO), 10mmol/L SB202190-monohydrochloride (Sigma-Aldrich), R-spondin-1 (RSPO1), Noggin, Wnt3a, 50ng/mL EGF (ThermoFisher) and penicillin/streptomycin (Sigma-Aldrich). To perform SQLE knockout, organoids were digested into single cells and infected with SQLE Lenti-sgControl or sgSQLE for 1h under centrifugation (600g), followed by 6h incubation at 37°C. Infected organoids were selected with puromycin (2μg/ml) for 2 weeks. SQLE knockout was confirmed by Western blot. For drug treatment, organoids were cultured in culture medium containing 60μM terbinafine for 6 days, with the medium renewed every 2 days.

Cell invasion assay

Cell invasion was performed using 8μm transwell plates and layered with 100μL of BD Matrigel™ matrix (1:6 dilution) for 30mins at 37°C. Cells (5×10^4/ml in 100ul FBS free medium) were added to the upper chamber, while 700μl of complete DMEM was added to the lower chamber. 16-24h later, the cells were fixed with 4% paraformaldehyde for 30min and stained with 1% crystal violet solution for 15min. Cells were counted under a light microscope. All experiments were conducted three times in triplicate.

Cell migration assay

For cell migration assay, cells (5×10^5) were seeded into a 6-well plates overnight. Then, the monolayers were scratched with a sterile 200μl tip. The width of the wounded area was captured using a microscope microscopy (Nikon, Tokyo, Japan) at 0 and 48 h. The

wound closure was measured with ImageJ software. All experiments were conducted three times in triplicate.

MTT assay

For cell viability assays, cells were seeded in a 96-well plate and MTT assay (5mg/ml; Promega) was performed according to the manufacturer's instruction. All experiments were conducted three times in triplicate.

Apoptosis and cell cycle analyses

For cell apoptosis, cells were analyzed 48h after seeding into 6-well plates. Apoptosis was assessed using the annexin-phycoerythrin/7-aminoactinomycin D staining kit (BD Biosciences). For cell cycle analysis, cells were serum-starved overnight and stimulated with complete medium for 4 to 8 hours. Cells were fixed in 70% ethanol, stained with propidium iodide, and analyzed by flow cytometry. All experiments were conducted three times in triplicate.

Germ-free mice

Germ-free C57/BL6 mice at 6 weeks old were divided into 2 groups (9 per group). One group of mice were fed with stools collected from Sqle tg mice and the other group of mice were fed with stools collected from corresponding wildtype mice. Briefly, stool samples (1g) was homogenized in 5mL of sterile PBS. Then, the germ-free mice were transplanted with 200μL of the suspension using gastric gavage (twice a week). One

Li C, *et al. Gut* 2022;0:1–13. doi: 10.1136/gutjnl-2021-325851

month later mice were sacrificed for further analysis.

Immunohistochemistry staining

Paraffin slides were used for analyzing SQLE and Ki67 (1:100 dilution) protein levels. The proportion of SQLE-positive cells was determined by counting at least 1000 cells in 5 random microscopic fields for each sample. SQLE immunoreactivity was analyzed in a semi-quantitative manner by two independent pathologists, who were blinded to outcome. The intensity of immunohistochemical stain was scored from 0-10 (0: 0-10% of positive cells; 1:10%-20% positive cells; 3: 20%-30% positive cells; 4: 30%-40% positive cells; 5: 40%-50% positive cells; 6:50%-60% positive cells; 7: 60%-70% positive cells; 8:70%-80% positive cells; 9:80%-90% positive cells; 10: 90%-100% positive cells). To identify the strong or weak of SQLE expression in microarray tissues, nuclear staining higher than 10% was defined as moderate/strong (high), whereas lower than 10% was defined as negative/weak (low). The signal of Ki-67–positive cells was determined by counting positive cells in crypts (5 random microscopic fields).

TUNEL staining

TUNEL staining was determined on paraffin slides using the DeadEnd Colorimetric TUNEL System (Promega). Briefly, paraffin in slides was removed by xylene and fixed in 4% paraformaldehyde in PBS. Next, TdT reaction mix was added to tissue sections and incubated for 60min at 37°C in a humidified chamber. Streptavidin horseradish peroxidase (1:500 in PBS) was then added, followed by 100ul of 3,3′-diaminobenzidine

for detection.

Metabolomics profiling

Stool samples (100mg) were dissolved in 500μL of ice-cold water, vortexed and centrifuged for 15min with 10,000g. Pellets were further extracted with 500μL cold methanol. Supernatants were combined for analysis. Chromatographic analyses were performed on a Waters Acquity UPLC system equipped with a BEHC18 column (Milford, USA). The mobile phases consisted of solvents A and B. The elution gradient program for fecal samples was: 0–1% B for 0.5 min; 1–30% B from 0.5 to 5 min; 30–50% B from 5 to 13 min and 50–100% B from 13 to 17 min; the flow rate was 0.45 mL/min. Mass spectra was obtained in a Waters SYNAPT G2 HDMS (Waters Corp., Manchester, UK) TOF mass spectrometer combined with an ESI source with positive ion scan mode. TOF parameters are as follow: capillary voltage: 3.0 KV; sample and extraction cone voltage: 40 V and 4.0 V; desolvation gas rate and temperature: 800 L/h and 400 °C; cone gas rate: 40 L/h; source temperature: 100 °C; scan time and inter scan delay: 0.15 and 0.02s. The lock mass in all analyses was leucine-enkephalin ([M+H]+ = 556.2771) with a concentration of 0.5μg/mL and a flow rate of 10μL/min. Raw data were acquired using centroid mode; the mass range was set from m/z 50 to m/z 1200. Metabolomic data was analyzed using R package Metabo AnalystR[20]. Altered metabolites were determined by a pair-wise comparison using Wilcoxon rank-sum test, with p-values adjusted by Benjamini-Hochberg false-discovery rate. Metabolites with adjusted $P<0.1$ and Log2(fold change)> 1 were considered significantly altered. Pair-

wise species-metabolites correlation coefficients were computed using Spearman's rank correlation coefficients (Spearman's rho). The strong correlation was determined by the cutoff |Spearman's rho| > 0.6 and P<0.025. All the heatmaps were plotted using R Package Complex Heatmap.

Li C, *et al. Gut* 2022;0:1–13. doi: 10.1136/gutjnl-2021-325851

Table S1. Clinicopathological features of CRC patients in Hong Kong cohort

Variables	SQLE expression (log2 of mRNA expression)	P value
Age		
≥60 (N=73) (50.6%)	1.158	0.377
<60 (N=71) (49.4%)	1.257	
Gender		
Male (N=81) (56.3%)	1.329	0.503
Female (N=63) (43.7%)	1.051	
Tumor site		
Colon (N=75) (52.1%)	1.023	0.051
Rectum (N=69) (47.9%)	1.409	
Differentiation		
High/moderate (N=104) (72.2%)	1.119	0.858
Low (N=40) (27.8%)	1.187	
TNM stage		
I+II (N=60) (41.7%)	0.977	0.019 *
III+IV (N=84) (58.3%)	1.782	
Metastasis		
Yes (N=45) (31.3%)	1.673	0.036 *
No (N=99) (68.7%)	1.051	

Table S2. Clinicopathological features of CRC patients in tissue microarray cohort

Variables	SQLE expression		P value
	Strong (n, %)	Weak (n, %)	
Age			
≥67 (N=106) (51.6%)	49 (46.2%)	57 (53.8%)	0.539
<67 (N=101) (48.4%)	51 (50.4%)	50 (49.6%)	
Gender			
Male (N=117) (56.5%)	57(48.7%)	60 (51.3%)	0.893
Female (N=90) (43.5%)	43 (47.8%)	47 (52.2%)	
Grade			
Well/Moderate (N=194) (93.7%)	94 (48.5%)	100 (51.5%)	0.872
Poor (N=13) (6.3)	6 (46.1%)	7 (53.9%)	
LN metastasis			
N0 (N=96) (46.4%)	19 (19.8%)	77 (81.2%)	0.002 **
N1 (n=68) (32.8%)	38 (55.9%)	30 (44.1%)	
N2 (n=43) (20.8%)	37 (86.0%)	6 (14%)	
Distance Metastasis			
M0 (N=142) (68.6%)	50 (35.2%)	92 (64.8%)	<0.0001****
M1 (N=65) (31.4%)	50 (76.9%)	15 (23.1%)	
Size (cm in diameter)			
≥4.5 (N=127) (61.4%)	62 (48.8%)	65 (51.2%)	0.111
<4.5 (N=80) (38.6%)	30 (37.5%)	50 (62.5%)	
AJCC stage			
1+2 (N=82) (39.6%)	26 (31.7%)	50 (68.3%)	0.002 **
3+4 (N=125) (60.4%)	74 (59.2%)	57 (40.8%)	
MSI			
MSS (n=194) (93.7%)	93 (93%)	101 (94.4%)	0.778
MSI-H (n=13) (6.3%)	7 (7%)	6 (5.6%)	

Table S3 Clinicopathological features of CRC patients in GSE17538 cohort

Variables	SQLE expression (log2 of mRNA expression)	P value
Age		0.659
≥65 (n=122)	5.428	
<65 (n=110)	5.427	
Gender		0.219
Male (n=122)	5.492	
Female (n=110)	5.395	
Differentiation		0.553
High and moderate (n=183)	5.411	
Low (n=30)	5.487	
AJCC stage		0.025 *
I+II (n=100)	5.031	
III+IV (n=132)	5.639	

Li C, *et al. Gut* 2022;0:1–13. doi: 10.1136/gutjnl-2021-325851

Table S4. List of primers

Gene	Primer	Sequence
Muc2	Forward	GCCCGTGGAGTCGTACGTGC
	Reverse	TTGGGGCAGAGTGAGGCGGT
Ki67	Forward	GTGCTGACCCTGATGGGGAAGG
	Reverse	GCTCTTGCCCTGCCTGACACC
Gapdh	Forward	CCCTTAAGAGGGATGCTGCC
	Reverse	ACTGTGCCGTTGAATTTGCC
SQLE	Forward	GATGATGCAGCTATTTTCGAGGC
	Reverse	CCTGAGCAAGGATATTCACGACA
GAPDH	Forward	CTTCACCACCATGGAGGAGGC
	Reverse	GGCATGGACTGTGGTCATGAG
DHCR7	Forward	CGCAGGACTTTAGCCGGT
	Reverse	TGTCATTGGTGACGCCATCT
DHCR24	Forward	TGAAGACAAACCGAGAGGGC
	Reverse	CAGCCAAAGAGGTAGCGGAA
FDFT1	Forward	CCACCCCGAAGAGTTCTACAA
	Reverse	TGCGACTGGTCTGATTGAGATA
FDPS	Forward	CAGCTTTCTACTCCTTCTACCTTCC
	Reverse	GCTCCTTCTCGCCATCAAT
HMGCR	Forward	TGATTGACCTTTCCAGAGCAAG
	Reverse	CTAAAATTGCCATTCCACGAGC
HMGCS1	Forward	CATTAGACCGCTGCTATTCTGTC
	Reverse	TTCAGCAACATCCGAGCTAGA
IDI1	Forward	TGGATAAAACCCCTGTGGTG
	Reverse	CAACATCCGGCATAACTGTG
LDLR	Forward	TACAAGTGGGTCTGCGATGG
	Reverse	TGAAGTCCCCGGATTTGCAG
MVD	Forward	GTAAGTGGCTGTGGAGCTGG
	Reverse	GGAGTTGATGGGCAGAACCA
MVK	Forward	CTCTGATTGGCTGGCCTGAA
	Reverse	CCAACTCCCACAACCCAGAG
PMVK	Forward	GCTGATGTCTGTGCTGTCCT
	Reverse	GAAAGGCCTCCTTGTAGGTG

Table S5. List of antibodies

Antibodies	Cat. Number	Company
SQLE	12544-1-AP	Proteintech
JAM-C	Ab81331	Abcam
Occlaudin	33-1500	Invitrogen
Caspase-3	9665s	Cell signaling
Cleaved Caspase-3	9661s	Cell signaling
Caspase-7	9492s	Cell signaling
Cleaved Caspase-7	9491s	Cell signaling
P53	Sc126	Santa Cruz
Cyclin D1	2922s	Cell signaling
PCNA	2586	Cell signaling
P21	Sc6246	Santa Cruz
PARP	Sc8007	Santa Cruz
Cleaved PARP	5625	Cell signaling
CDK4	12790	Cell signaling
$p27^{Kip1}$	3686	Cell signaling
GAPDH	Sc4772	Santa Cruz
HMGCR	A1633	ABclonal
FDPS	A5744	ABclonal
FDFT1	A4651	ABclonal

Li C, *et al. Gut* 2022;0:1–13. doi: 10.1136/gutjnl-2021-325851

Table S6. List of primers for specific bacteria

Gene name	Primers	Sequence
Brucella abortus	Forward	CATGCGCTATGTCTGGTTAC
	Reverse	GGCTTTTCTATCACGGTATTC
Desulfovibrio fairfieldensis (CP014229.1)	Forward	GGCAACAGCCTGGTTATGAT
Hypothetical protein	Reverse	ACGAAGATGGACGAAAGCAT
Rhodococcus erythropolis (CP050124.1)	Forward	AGCACATATCGACCCAGGAC
Non-ribosomal peptide synthetase	Reverse	CGAGGTGAAAGTGCAGATCA
Chlamydia muridarum (NZ_CP009760.1)	Forward	GCGACGCATATGTTCGGAGA
ABC transporter substrate-binding protein	Reverse	TGTGCTGAGGTTGGGACTTG
Streptomyces violaceusniger (CP002994.1)	Forward	AGGTCGCCCTCAGCTCTC
TPR-repeat protein	Reverse	AACGGGATCAGGGGTAGGT
Pseudomonas sp. Leaf58 (NZ_CP032677.1)	Forward	CGTGGTGCTGTCGCTACTAC
MSF transporter	Reverse	CAAGCCAATACCAATCGACA
Universe QPCR-Eub341F	Forward	ACTCCTACGGGAGGCAGCAGT
Universe QPCR-Eub534R	Reverse	ATTACCGCGGCTGCTGGC

Reference:

1. Redkar R, Rose S, Bricker B, DelVecchio V. Real-time detection of Brucella abortus, Brucella melitensis and Brucella suis. ***Mol Cell Probes***. 2001 Feb;15(1):43-52.

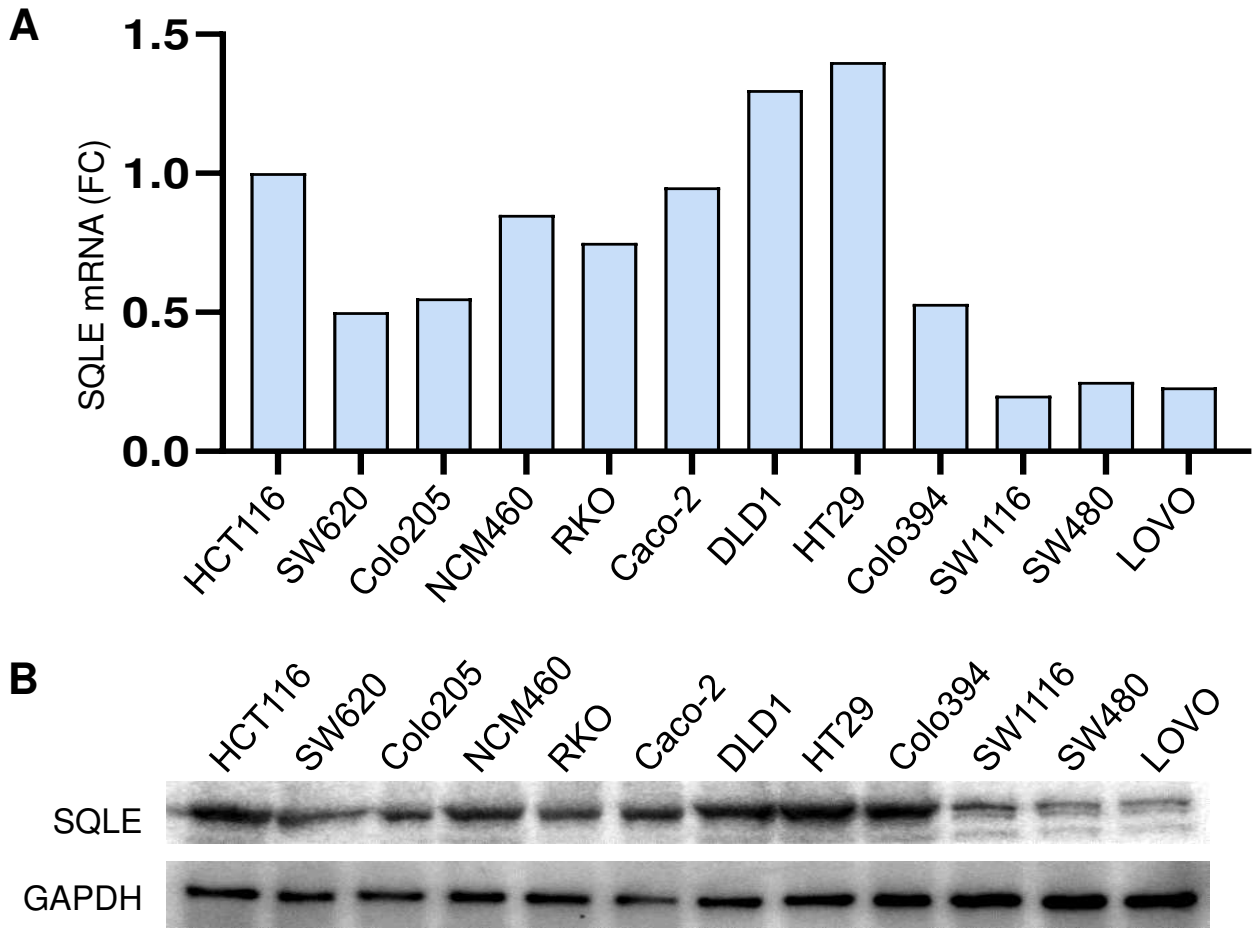

Figure S1. SQLE mRNA (**A**) and protein (**B**) expression was determined by qPCR and Western blot.

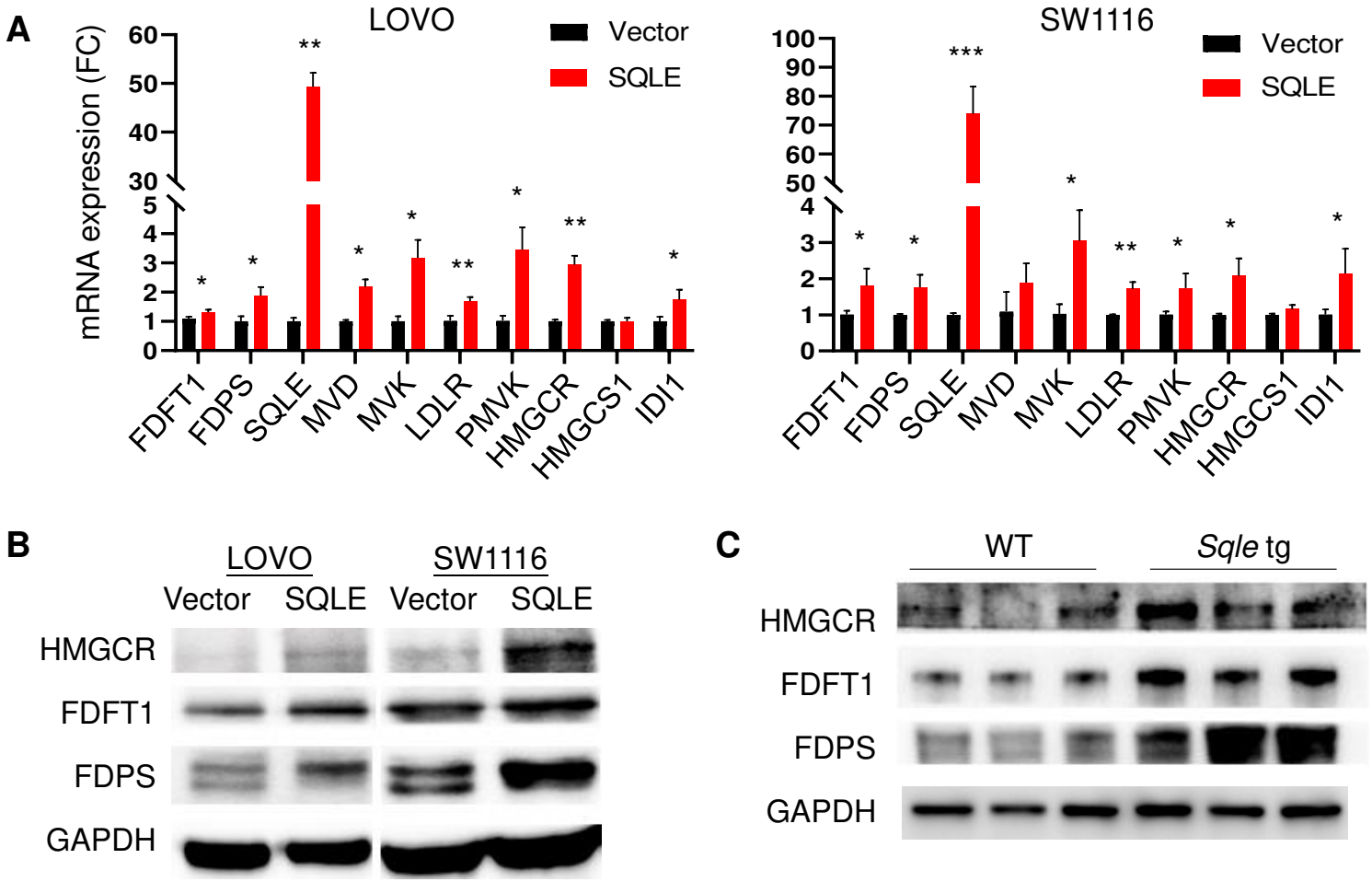

Figure S2. SQLE overexpression promotes genes of cholesterol biosynthesis pathway in **(A)** CRC cell lines by qPCR (**A**) and Western blot (**B**), and in colon-specific *Sqle* tg mice by Western blot (C).

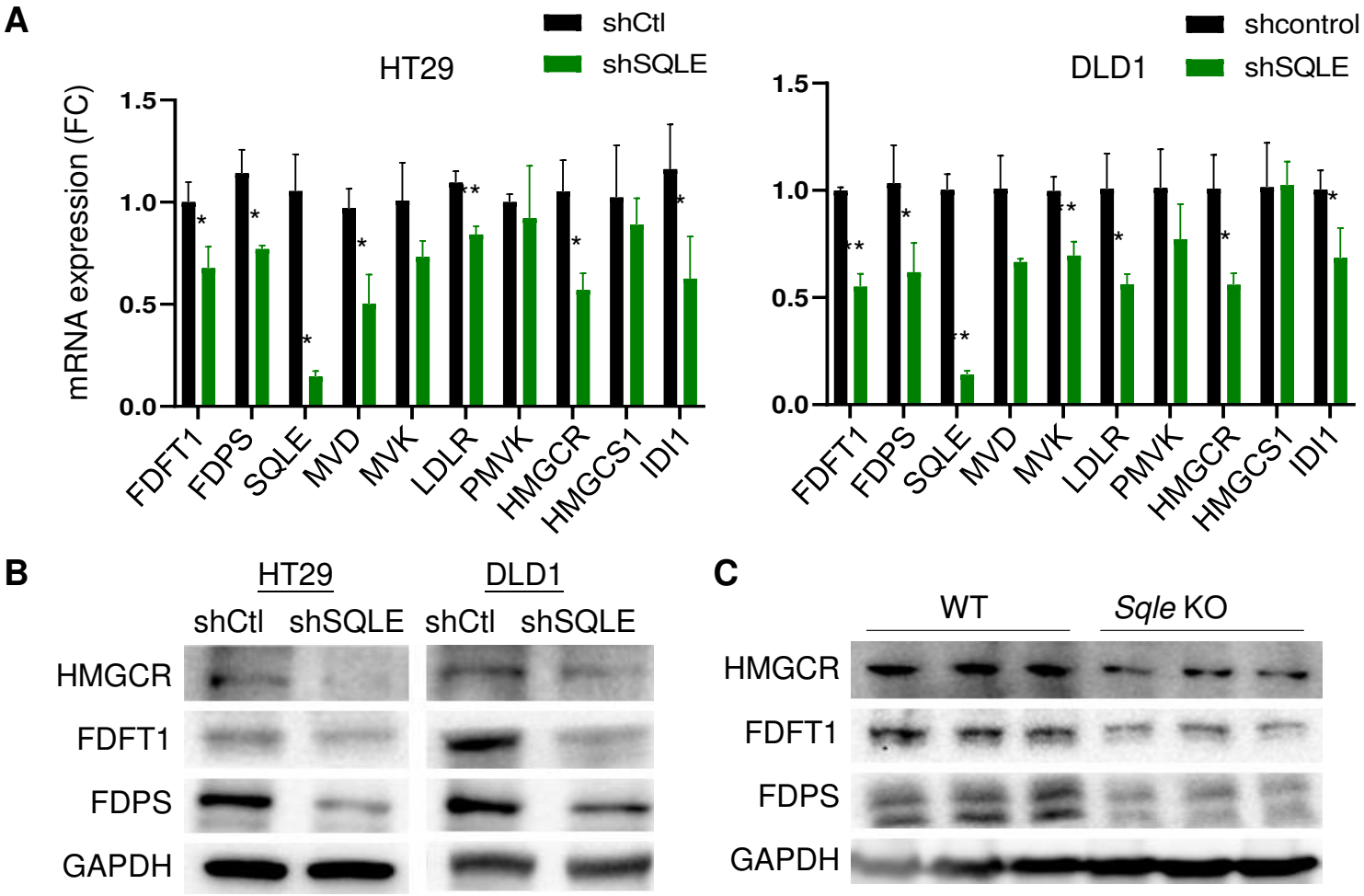

Figure S3. SQLE knockdown inhibits genes of cholesterol biosynthesis pathway in **(A)** CRC cell lines by qPCR (**A**) and Western blot (**B**), and in colon-specific *Sqle* tg mice by Western blot (C).

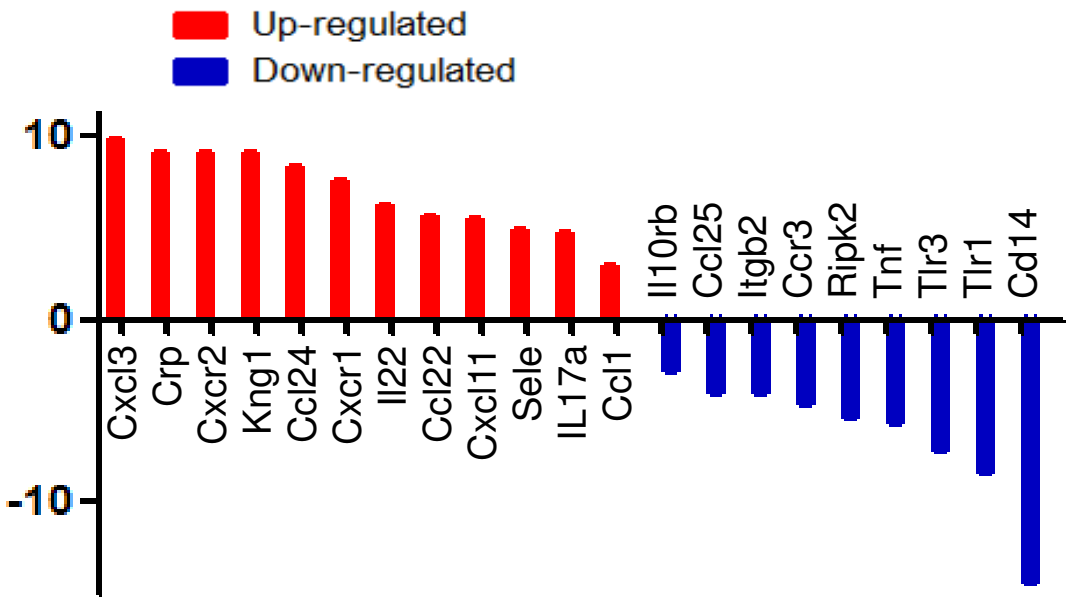

Figure S4. Inflammation pathway PCR array analysis of the colon tissues from Sqle tg mice and wildtype littermates.

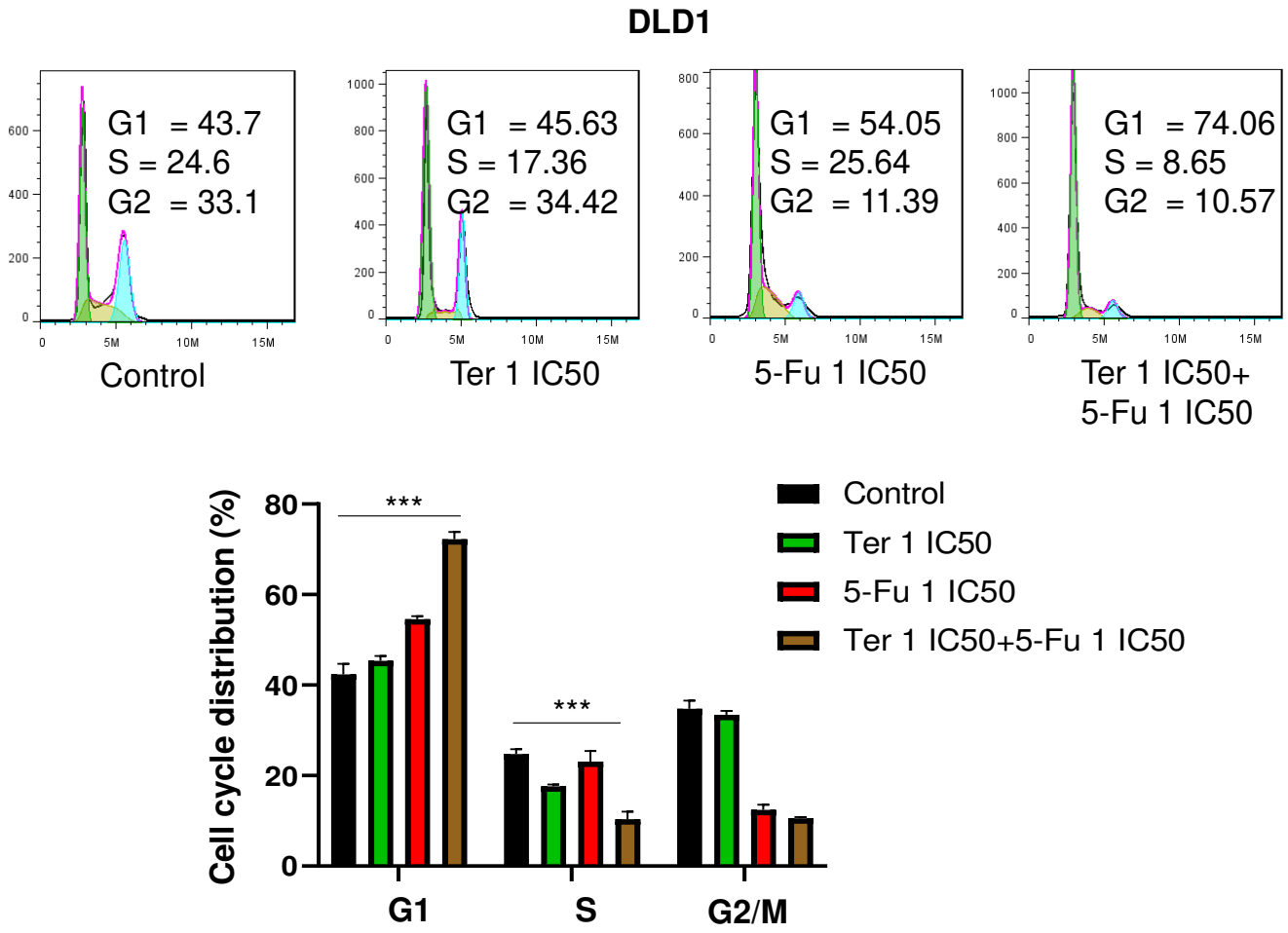

Figure S5. Terbinafine in combination with 5-FU synergistically induced G1 cell cycle arrest in DLD1 cells.

Supplementary Methods

Human CRC cancer cell lines

SW1116, LOVO, HT29 and DLD1 cells were purchased from the American Type Culture Collection (ATCC, Manassas, VA) and grown in DMEM supplemented with 10% fetal bovine serum (FBS) and antibiotics. All cell lines were cultured at 37°C in an incubator with 95% air and 5% CO_2 supply.

RNA extraction, semi-quantitative RT-PCR, and real-time PCR analyses

Total RNA was extracted from cells and tissues using TRIzol™. cDNA was synthesized from 1μg of total RNA using Transcriptor Reverse Transcriptase (Roche). Real-time PCR was performed using SYBR Green master mix (Roche) on LightCycler 480. Each sample was performed in triplicate. ΔΔCT method was applied to determine the fold change in gene expression. Primer sequences are listed in **Table S4**.

Plasmids and gene transfection

pCMV-SQLE (RC202008), pCMV control plasmids, SQLE shRNA (TL309122V), and control shRNA (pGFP-C-shLenti) plasmids were ordered from OriGene. pCMV control and pCMV-SQLE plasmids were transfected into CRC cells using Lipofectamine 2000 (Invitrogen). For stable cell lines selection, cells were passed into fresh growth medium with 800mg/ml neomycin (G418). After one month of selection, cells were harvested to detect SQLE expression. For shRNA, lentivirus was generated using HEK293T cells by transfection of shRNA plasmid with packaging plasmids. After 72h post-transfection,

the culture supernatants were used for transduction of CRC cells. For stable cell lines selection, cells were passed into fresh growth medium with 2μg/ml puromycin. After 2 weeks of selection, cells were harvested to detect SQLE expression.

Western blot

20-40 mg protein was loaded onto 12% SDS-PAGE and transferred to an equilibrated polyvinylidenedifluoride (PVDF) membrane (Invitrogen). After blocking in 5% BSA dissolved in TBST solution at room temperature for 1h, the membrane was incubated with primary antibody in 5% BSA overnight at 4°C. After washing steps, the membrane was incubated with secondary antibody for 1h at room temperature. After 4 washing steps, protein was detected by enhanced chemiluminescence reagent (ECL, Amersham Corporation, Heights, IL, USA). Antibodies used in this study are shown in **Table S5**.

Colony formation assay

For the cell colony formation assay, stably transfected cells (1000/well) were plated in 6-well plates. After culturing for 7 days, cells were fixed with 70% ethanol and stained with 0.25% crystal violet solution. Colonies with over 50 cells per colony were counted. All experiments were conducted three times in triplicate.

Transmission Electron Microscopy

Small pieces of colon tissues (1mm^3) from germ-free mice (fed with stools from Sqle tg mice or wildtype mice) were collected and fixed in 2.0% glutaraldehyde in 0.1 mol/L

sodium cacodylate (Electron Microscopy Sciences, Hatfield, PA). The ultrathin sections were prepared on a Reichert Ultracut E ultramicrotome, and examined using a Philips CM100 transmission electron microscope.

Microbial DNA Extraction and Bacteria Quantification

DNA was extracted from mice stools using the DNeasy PowerSoil Kit (QIAGEN) according to the manufacturer's instructions. For qPCR quantification of differentially expressed bacteria, genomic DNA was amplified by qPCR with universal SYBR Green PCR Master Mix (Takara) on the ABI QuantStudio 7 Flex Real-Time PCR System, and normalized to 16S gene abundance. Primers used for detecting specific bacteria species are listed in **Table S6**. For *Desulfovibrio Fairfieldensis*, *Rhodococcus erythropolis*, *Chlamydia muridarum*, *Streptomyces violaceusniger*, *Pseudomonas sp.* Leaf58, primer was designed using NCBI/Genebank. When target Genebank sequences were chosen, "pick primers" was applied (nr database and Bacteria organism). Specificity of primers was examined using NCBI/Primer-Blast to confirm that no off-target bacteria could be amplified by the primers. Genebank numbers and targeted proteins were listed in **Table S6**. For *Brucella abortus*, the primer sequences were reported previously [1] and its specificity was confirmed using NCBI/Primer-Blast.

Patient-derived CRC organoids

Primary CRC organoids (CRC-816, CRC-828) were obtained from Princess Margaret Living Biobank (Canada), and cultured in DMEM/F12 with N2 and B27 supplements

(ThermoFisher), 10mmol/L HEPES, 1.25mmol/L N-acetyl cysteine (Sigma-Aldrich, St Louis, MO), 10mmol/L SB202190-monohydrochloride (Sigma-Aldrich), R-spondin-1 (RSPO1), Noggin, Wnt3a, 50ng/mL EGF (ThermoFisher) and penicillin/streptomycin (Sigma-Aldrich). To perform SQLE knockout, organoids were digested into single cells and infected with SQLE Lenti-sgControl or sgSQLE for 1h under centrifugation (600g), followed by 6h incubation at 37°C. Infected organoids were selected with puromycin (2μg/ml) for 2 weeks. SQLE knockout was confirmed by Western blot. For drug treatment, organoids were cultured in culture medium containing 60μM terbinafine for 6 days, with the medium renewed every 2 days.

Cell invasion assay

Cell invasion was performed using 8μm transwell plates and layered with 100μL of BD Matrigel™ matrix (1:6 dilution) for 30mins at 37°C. Cells (5×10^4/ml in 100ul FBS free medium) were added to the upper chamber, while 700μl of complete DMEM was added to the lower chamber. 16-24h later, the cells were fixed with 4% paraformaldehyde for 30min and stained with 1% crystal violet solution for 15min. Cells were counted under a light microscope. All experiments were conducted three times in triplicate.

Cell migration assay

For cell migration assay, cells (5×10^5) were seeded into a 6-well plates overnight. Then, the monolayers were scratched with a sterile 200μl tip. The width of the wounded area was captured using a microscope microscopy (Nikon, Tokyo, Japan) at 0 and 48 h. The

wound closure was measured with ImageJ software. All experiments were conducted three times in triplicate.

MTT assay

For cell viability assays, cells were seeded in a 96-well plate and MTT assay (5mg/ml; Promega) was performed according to the manufacturer's instruction. All experiments were conducted three times in triplicate.

Apoptosis and cell cycle analyses

For cell apoptosis, cells were analyzed 48h after seeding into 6-well plates. Apoptosis was assessed using the annexin-phycoerythrin/7-aminoactinomycin D staining kit (BD Biosciences). For cell cycle analysis, cells were serum-starved overnight and stimulated with complete medium for 4 to 8 hours. Cells were fixed in 70% ethanol, stained with propidium iodide, and analyzed by flow cytometry. All experiments were conducted three times in triplicate.

Germ-free mice

Germ-free C57/BL6 mice at 6 weeks old were divided into 2 groups (9 per group). One group of mice were fed with stools collected from Sqle tg mice and the other group of mice were fed with stools collected from corresponding wildtype mice. Briefly, stool samples (1g) was homogenized in 5mL of sterile PBS. Then, the germ-free mice were transplanted with 200μL of the suspension using gastric gavage (twice a week). One

Li C, *et al. Gut* 2022;0:1–13. doi: 10.1136/gutjnl-2021-325851

month later mice were sacrificed for further analysis.

Immunohistochemistry staining

Paraffin slides were used for analyzing SQLE and Ki67 (1:100 dilution) protein levels. The proportion of SQLE-positive cells was determined by counting at least 1000 cells in 5 random microscopic fields for each sample. SQLE immunoreactivity was analyzed in a semi-quantitative manner by two independent pathologists, who were blinded to outcome. The intensity of immunohistochemical stain was scored from 0-10 (0: 0-10% of positive cells; 1:10%-20% positive cells; 3: 20%-30% positive cells; 4: 30%-40% positive cells; 5: 40%-50% positive cells; 6:50%-60% positive cells; 7: 60%-70% positive cells; 8:70%-80% positive cells; 9:80%-90% positive cells; 10: 90%-100% positive cells). To identify the strong or weak of SQLE expression in microarray tissues, nuclear staining higher than 10% was defined as moderate/strong (high), whereas lower than 10% was defined as negative/weak (low). The signal of Ki-67–positive cells was determined by counting positive cells in crypts (5 random microscopic fields).

TUNEL staining

TUNEL staining was determined on paraffin slides using the DeadEnd Colorimetric TUNEL System (Promega). Briefly, paraffin in slides was removed by xylene and fixed in 4% paraformaldehyde in PBS. Next, TdT reaction mix was added to tissue sections and incubated for 60min at 37°C in a humidified chamber. Streptavidin horseradish peroxidase (1:500 in PBS) was then added, followed by 100ul of 3,3′-diaminobenzidine

for detection.

Metabolomics profiling

Stool samples (100mg) were dissolved in 500μL of ice-cold water, vortexed and centrifuged for 15min with 10,000g. Pellets were further extracted with 500μL cold methanol. Supernatants were combined for analysis. Chromatographic analyses were performed on a Waters Acquity UPLC system equipped with a BEHC18 column (Milford, USA). The mobile phases consisted of solvents A and B. The elution gradient program for fecal samples was: 0–1% B for 0.5 min; 1–30% B from 0.5 to 5 min; 30–50% B from 5 to 13 min and 50–100% B from 13 to 17 min; the flow rate was 0.45 mL/min. Mass spectra was obtained in a Waters SYNAPT G2 HDMS (Waters Corp., Manchester, UK) TOF mass spectrometer combined with an ESI source with positive ion scan mode. TOF parameters are as follow: capillary voltage: 3.0 KV; sample and extraction cone voltage: 40 V and 4.0 V; desolvation gas rate and temperature: 800 L/h and 400 °C; cone gas rate: 40 L/h; source temperature: 100 °C; scan time and inter scan delay: 0.15 and 0.02s. The lock mass in all analyses was leucine-enkephalin ([M+H]+ = 556.2771) with a concentration of 0.5μg/mL and a flow rate of 10μL/min. Raw data were acquired using centroid mode; the mass range was set from m/z 50 to m/z 1200. Metabolomic data was analyzed using R package Metabo AnalystR[20]. Altered metabolites were determined by a pair-wise comparison using Wilcoxon rank-sum test, with p-values adjusted by Benjamini-Hochberg false-discovery rate. Metabolites with adjusted $P<0.1$ and Log2(fold change)> 1 were considered significantly altered. Pair-

wise species-metabolites correlation coefficients were computed using Spearman's rank correlation coefficients (Spearman's rho). The strong correlation was determined by the cutoff |Spearman's rho| > 0.6 and P<0.025. All the heatmaps were plotted using R Package Complex Heatmap.

Li C, *et al. Gut* 2022;0:1–13. doi: 10.1136/gutjnl-2021-325851

Table S1. Clinicopathological features of CRC patients in Hong Kong cohort

Variables	SQLE expression (log2 of mRNA expression)	P value
Age		
≥60 (N=73) (50.6%)	1.158	0.377
<60 (N=71) (49.4%)	1.257	
Gender		
Male (N=81) (56.3%)	1.329	0.503
Female (N=63) (43.7%)	1.051	
Tumor site		
Colon (N=75) (52.1%)	1.023	0.051
Rectum (N=69) (47.9%)	1.409	
Differentiation		
High/moderate (N=104) (72.2%)	1.119	0.858
Low (N=40) (27.8%)	1.187	
TNM stage		
I+II (N=60) (41.7%)	0.977	0.019 *
III+IV (N=84) (58.3%)	1.782	
Metastasis		
Yes (N=45) (31.3%)	1.673	0.036 *
No (N=99) (68.7%)	1.051	

Table S2. Clinicopathological features of CRC patients in tissue microarray cohort

Variables	SQLE expression		P value
	Strong (n, %)	Weak (n, %)	
Age			
≥67 (N=106) (51.6%)	49 (46.2%)	57 (53.8%)	0.539
<67 (N=101) (48.4%)	51 (50.4%)	50 (49.6%)	
Gender			
Male (N=117) (56.5%)	57(48.7%)	60 (51.3%)	0.893
Female (N=90) (43.5%)	43 (47.8%)	47 (52.2%)	
Grade			
Well/Moderate (N=194) (93.7%)	94 (48.5%)	100 (51.5%)	0.872
Poor (N=13) (6.3)	6 (46.1%)	7 (53.9%)	
LN metastasis			
N0 (N=96) (46.4%)	19 (19.8%)	77 (81.2%)	0.002 **
N1 (n=68) (32.8%)	38 (55.9%)	30 (44.1%)	
N2 (n=43) (20.8%)	37 (86.0%)	6 (14%)	
Distance Metastasis			
M0 (N=142) (68.6%)	50 (35.2%)	92 (64.8%)	<0.0001****
M1 (N=65) (31.4%)	50 (76.9%)	15 (23.1%)	
Size (cm in diameter)			
≥4.5 (N=127) (61.4%)	62 (48.8%)	65 (51.2%)	0.111
<4.5 (N=80) (38.6%)	30 (37.5%)	50 (62.5%)	
AJCC stage			
1+2 (N=82) (39.6%)	26 (31.7%)	50 (68.3%)	0.002 **
3+4 (N=125) (60.4%)	74 (59.2%)	57 (40.8%)	
MSI			
MSS (n=194) (93.7%)	93 (93%)	101 (94.4%)	0.778
MSI-H (n=13) (6.3%)	7 (7%)	6 (5.6%)	

Table S3 Clinicopathological features of CRC patients in GSE17538 cohort

Variables	SQLE expression (log2 of mRNA expression)	P value
Age		0.659
≥65 (n=122)	5.428	
<65 (n=110)	5.427	
Gender		0.219
Male (n=122)	5.492	
Female (n=110)	5.395	
Differentiation		0.553
High and moderate (n=183)	5.411	
Low (n=30)	5.487	
AJCC stage		0.025 *
I+II (n=100)	5.031	
III+IV (n=132)	5.639	

Table S4. List of primers

Gene	Primer	Sequence
Muc2	Forward	GCCCGTGGAGTCGTACGTGC
	Reverse	TTGGGGCAGAGTGAGGCGGT
Ki67	Forward	GTGCTGACCCTGATGGGGAAGG
	Reverse	GCTCTTGCCCTGCCTGACACC
Gapdh	Forward	CCCTTAAGAGGGATGCTGCC
	Reverse	ACTGTGCCGTTGAATTTGCC
SQLE	Forward	CTTCTCCTCAAAGCGAGCACA
	Reverse	TTATTTAAAAATCGCCTGCTGGA
GAPDH	Forward	CTTCACCACCATGGAGGAGGC
	Reverse	GGCATGGACTGTGGTCATGAG
DHCR7	Forward	CGCAGGACTTTAGCCGGT
	Reverse	TGTCATTGGTGACGCCATCT
DHCR24	Forward	TGAAGACAAACCGAGAGGGC
	Reverse	CAGCCAAAGAGGTAGCGGAA
FDFT1	Forward	CCACCCCGAAGAGTTCTACAA
	Reverse	TGCGACTGGTCTGATTGAGATA
FDPS	Forward	CAGCTTTCTACTCCTTCTACCTTCC
	Reverse	GCTCCTTCTCGCCATCAAT
HMGCR	Forward	TGATTGACCTTTCCAGAGCAAG
	Reverse	CTAAAATTGCCATTCCACGAGC
HMGCS1	Forward	CATTAGACCGCTGCTATTCTGTC
	Reverse	TTCAGCAACATCCGAGCTAGA
IDI1	Forward	TGGATAAAACCCCTGTGGTG
	Reverse	CAACATCCGGCATAACTGTG
LDLR	Forward	TACAAGTGGGTCTGCGATGG
	Reverse	TGAAGTCCCCGGATTTGCAG
MVD	Forward	GTAAGTGGCTGTGGAGCTGG
	Reverse	GGAGTTGATGGGCAGAACCA
MVK	Forward	CTCTGATTGGCTGGCCTGAA
	Reverse	CCAACTCCCACAACCCAGAG
PMVK	Forward	GCTGATGTCTGTGCTGTCCT
	Reverse	GAAAGGCCTCCTTGTAGGTG

Table S5. List of antibodies

Antibodies	Cat. Number	Company
SQLE	12544-1-AP	Proteintech
JAM-C	Ab81331	Abcam
Occlaudin	33-1500	Invitrogen
Caspase-3	9665s	Cell signaling
Cleaved Caspase-3	9661s	Cell signaling
Caspase-7	9492s	Cell signaling
Cleaved Caspase-7	9491s	Cell signaling
P53	Sc126	Santa Cruz
Cyclin D1	2922s	Cell signaling
PCNA	2586	Cell signaling
P21	Sc6246	Santa Cruz
PARP	Sc8007	Santa Cruz
Cleaved PARP	5625	Cell signaling
CDK4	12790	Cell signaling
$p27^{Kip1}$	3686	Cell signaling
GAPDH	Sc4772	Santa Cruz
HMGCR	A1633	ABclonal
FDPS	A5744	ABclonal
FDFT1	A4651	ABclonal

Li C, *et al. Gut* 2022;0:1–13. doi: 10.1136/gutjnl-2021-325851

Table S6. List of primers for specific bacteria

Gene name	Primers	Sequence
Brucella abortus	Forward	CATGCGCTATGTCTGGTTAC
	Reverse	GGCTTTTCTATCACGGTATTC
Desulfovibrio fairfieldensis (CP014229.1)	Forward	GGCAACAGCCTGGTTATGAT
Hypothetical protein	Reverse	ACGAAGATGGACGAAAGCAT
Rhodococcus erythropolis (CP050124.1)	Forward	AGCACATATCGACCCAGGAC
Non-ribosomal peptide synthetase	Reverse	CGAGGTGAAAGTGCAGATCA
Chlamydia muridarum (NZ_CP009760.1)	Forward	GCGACGCATATGTTCGGAGA
ABC transporter substrate-binding protein	Reverse	TGTGCTGAGGTTGGGACTTG
Streptomyces violaceusniger (CP002994.1)	Forward	AGGTCGCCCTCAGCTCTC
TPR-repeat protein	Reverse	AACGGGATCAGGGGTAGGT
Pseudomonas sp. Leaf58 (NZ_CP032677.1)	Forward	CGTGGTGCTGTCGCTACTAC
MSF transporter	Reverse	CAAGCCAATACCAATCGACA
Universe QPCR-Eub341F	Forward	ACTCCTACGGGAGGCAGCAGT
Universe QPCR-Eub534R	Reverse	ATTACCGCGGCTGCTGGC

Reference:

1. Redkar R, Rose S, Bricker B, DelVecchio V. Real-time detection of Brucella abortus, Brucella melitensis and Brucella suis. ***Mol Cell Probes***. 2001 Feb;15(1):43-52.

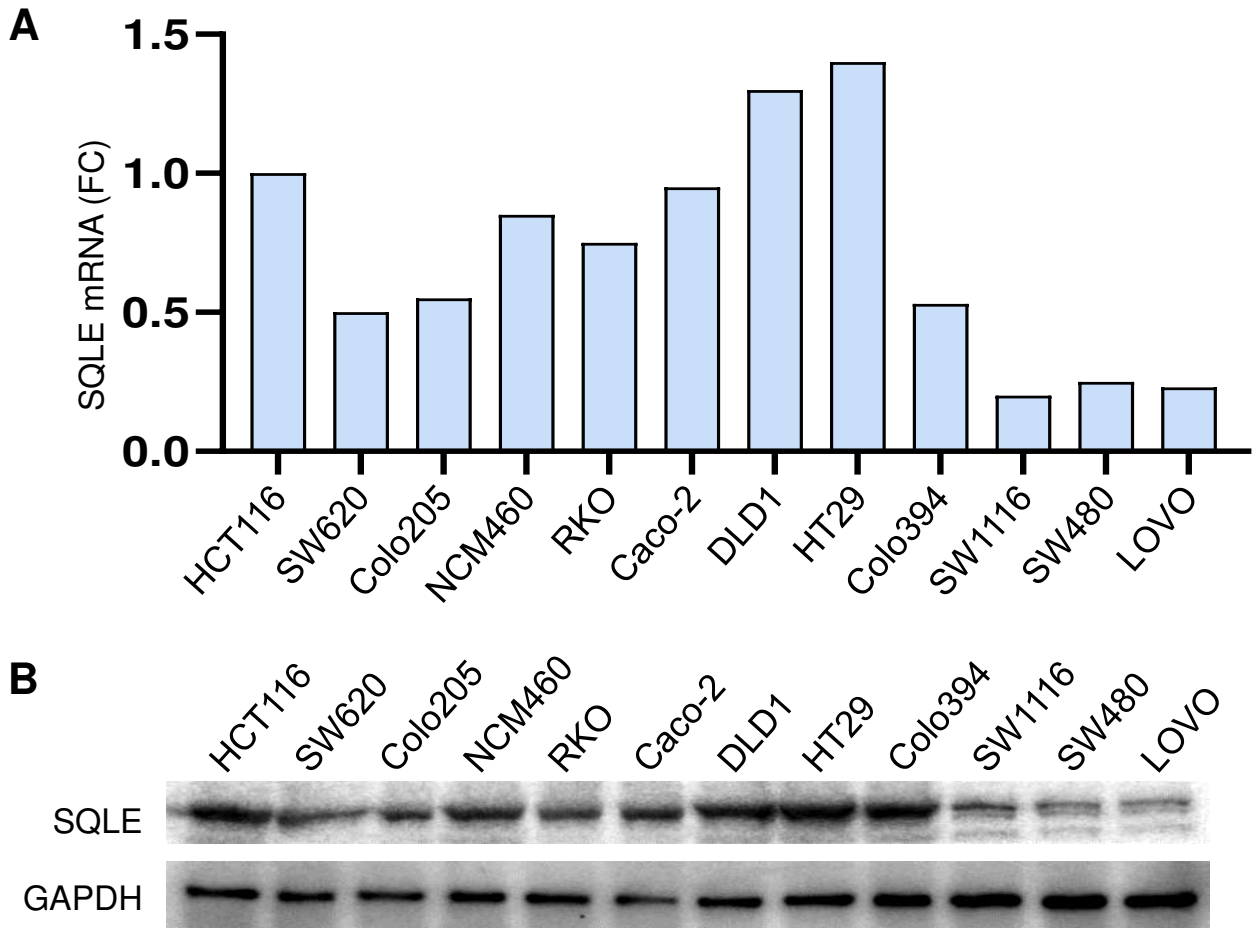

Figure S1. SQLE mRNA (**A**) and protein (**B**) expression was determined by qPCR and Western blot.

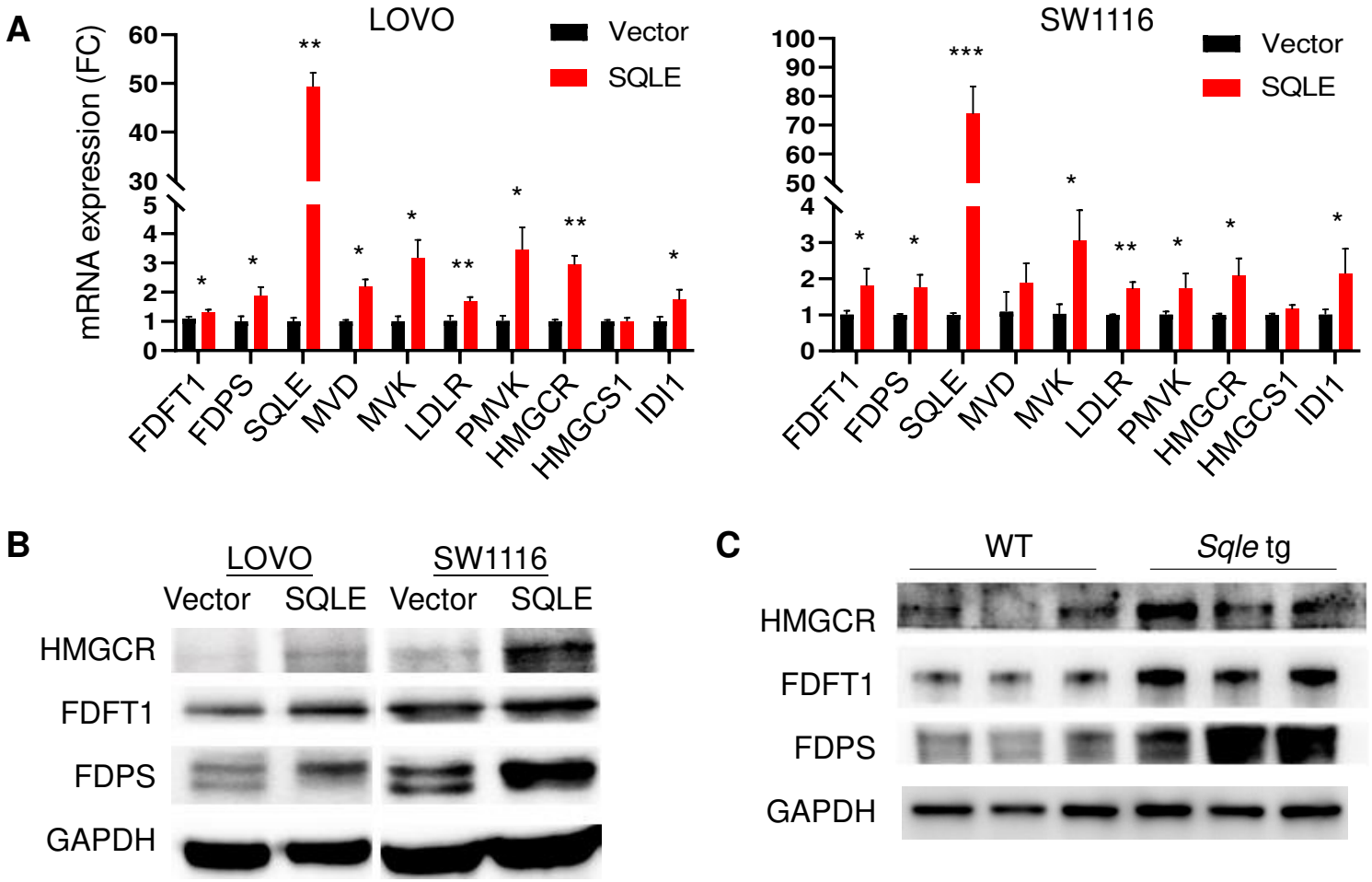

Figure S2. SQLE overexpression promotes genes of cholesterol biosynthesis pathway in **(A)** CRC cell lines by qPCR (**A**) and Western blot (**B**), and in colon-specific *Sqle* tg mice by Western blot (C).

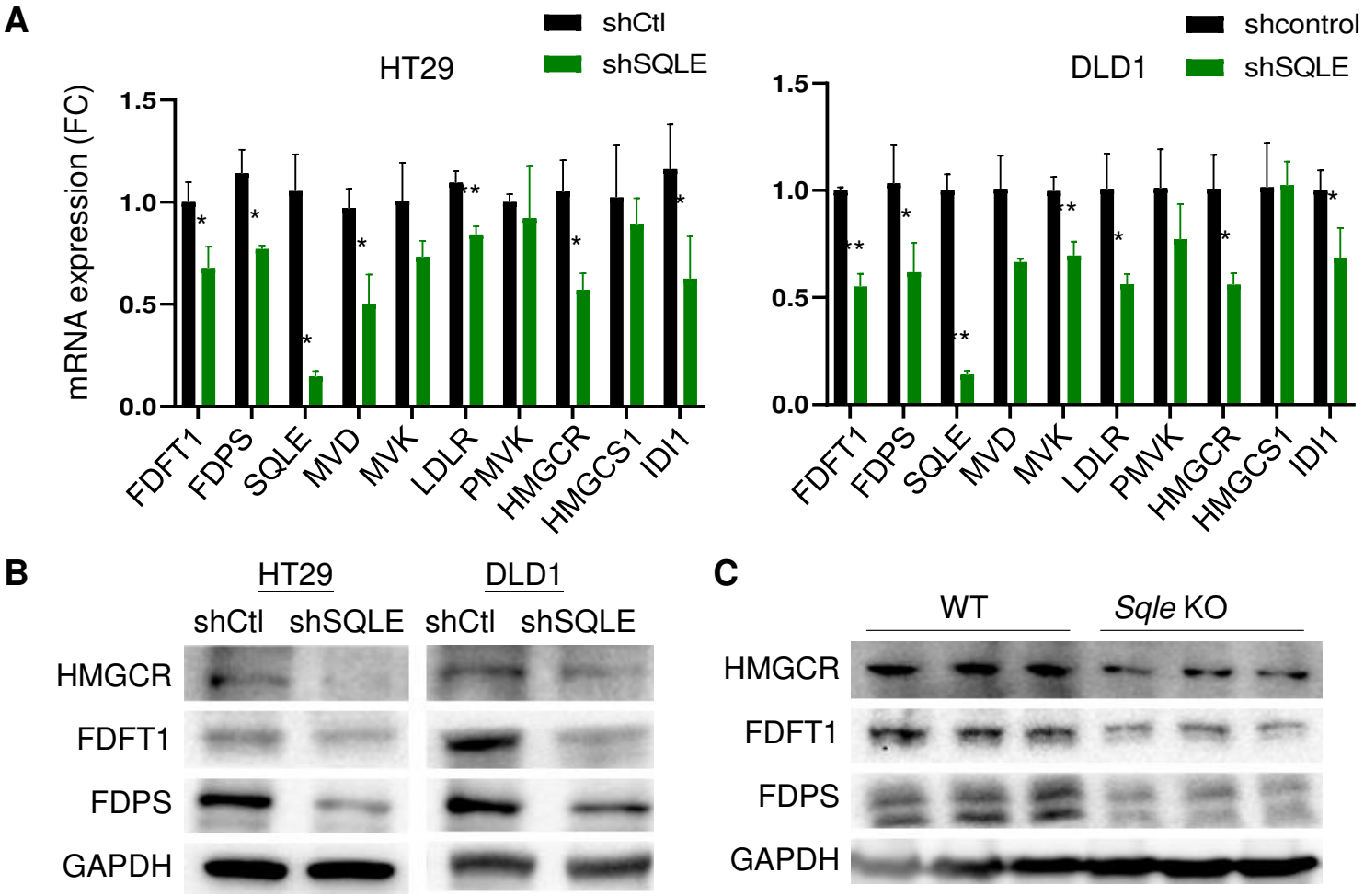

Figure S3. SQLE knockdown inhibits genes of cholesterol biosynthesis pathway in **(A)** CRC cell lines by qPCR (**A**) and Western blot (**B**), and in colon-specific *Sqle* tg mice by Western blot (C).

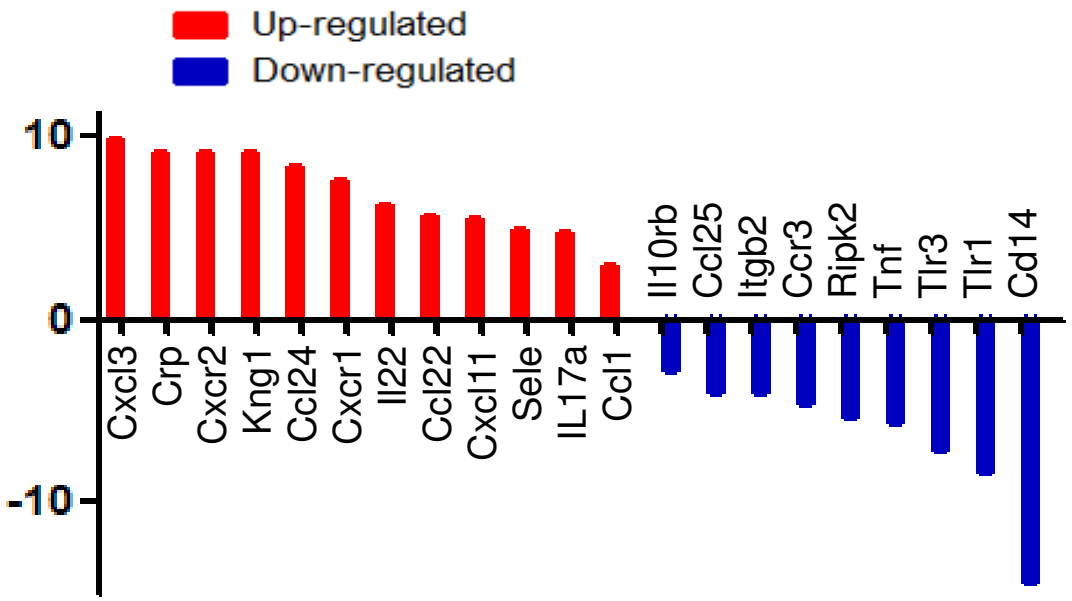

Figure S4. Inflammation pathway PCR array analysis of the colon tissues from Sqle tg mice and wildtype littermates.

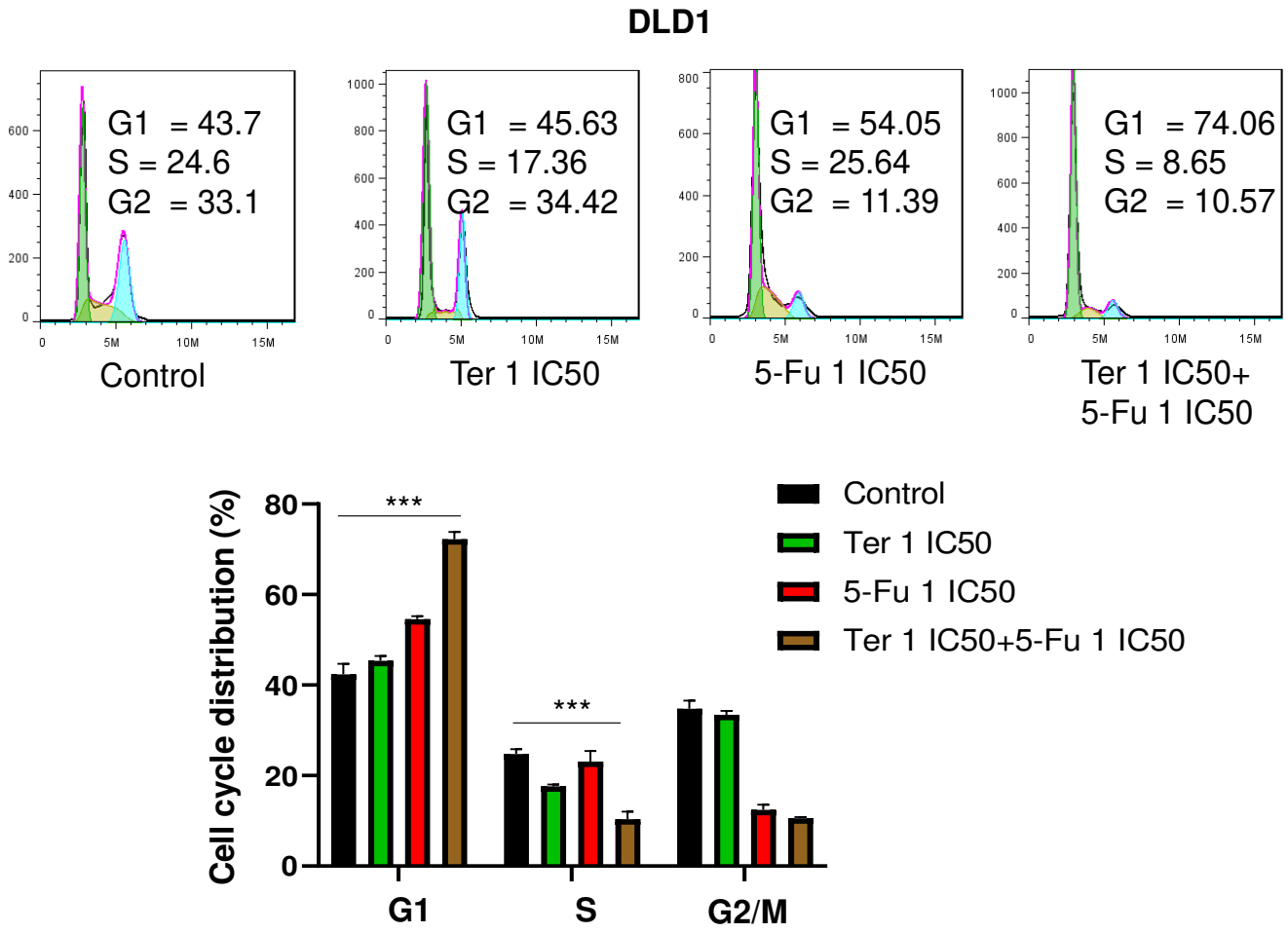

Figure S5. Terbinafine in combination with 5-FU synergistically induced G1 cell cycle arrest in DLD1 cells.